U.S. DEPARTMENT OF COMMERCE
National Technical Information Service

PB-273 359

Nonwoven Fabric Filters for Particulate Removal in Respirable Dust Range

Textile Research Inst, Princeton, N J

Prepared for

Industrial Environmental Research Lab, Research Triangle Park, N C

Oct 77

PB 273 359

EPA U.S. Environmental Protection Agency
Office of Research and Development
Industrial Environmental Research Laboratory
Research Triangle Park, North Carolina 27711

EPA-600/7-77-115
October 1977

NONWOVEN FABRIC FILTERS FOR PARTICULATE REMOVAL IN RESPIRABLE DUST RANGE

Interagency
Energy-Environment
Research and Development
Program Report

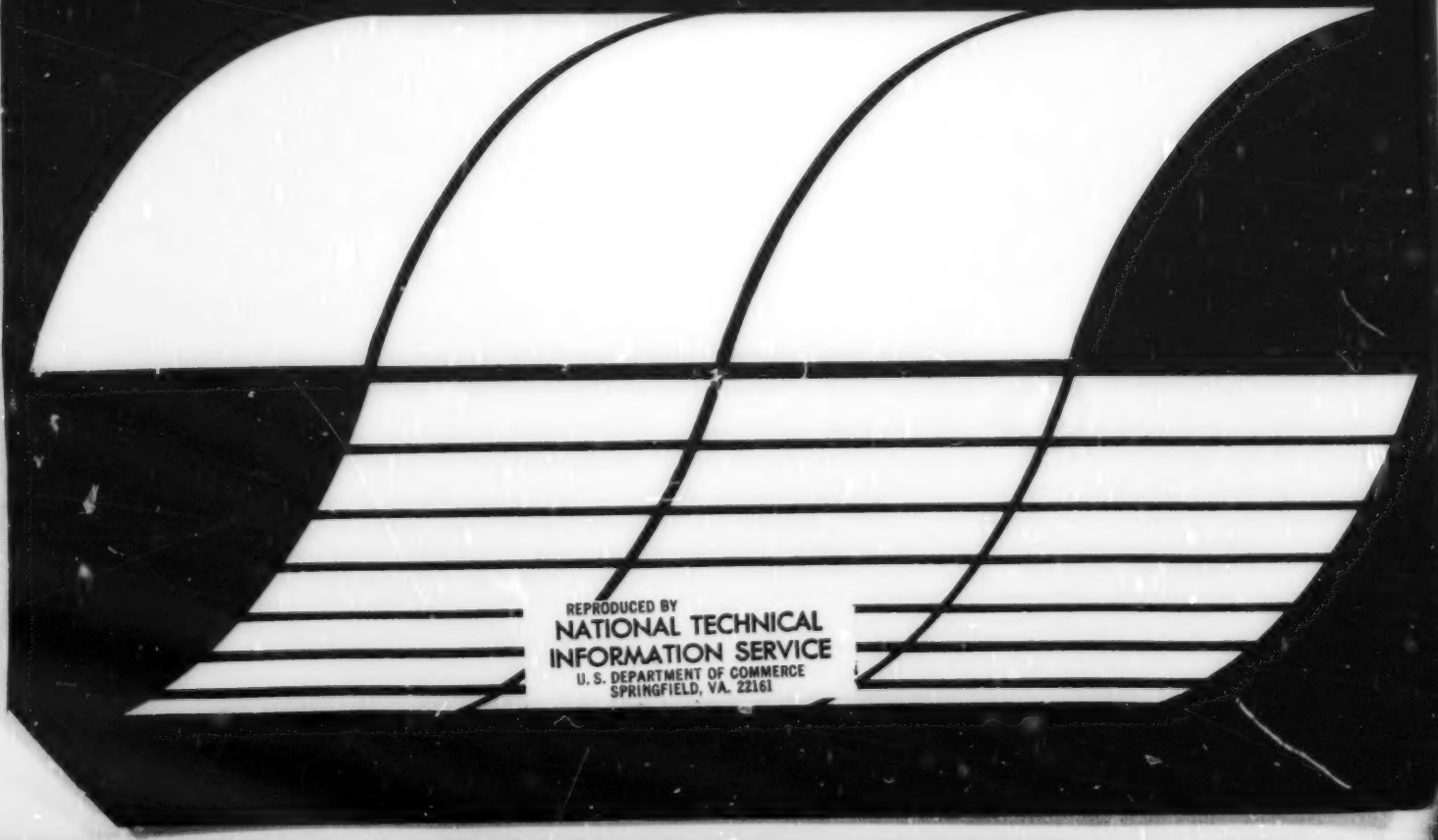

REPRODUCED BY
NATIONAL TECHNICAL
INFORMATION SERVICE
U.S. DEPARTMENT OF COMMERCE
SPRINGFIELD, VA. 22161

RESEARCH REPORTING SERIES

Research reports of the Office of Research and Development, U.S. Environmental Protection Agency, have been grouped into seven series. These seven broad categories were established to facilitate further development and application of environmental technology. Elimination of traditional grouping was consciously planned to foster technology transfer and a maximum interface in related fields. The seven series are:

1. Environmental Health Effects Research
2. Environmental Protection Technology
3. Ecological Research
4. Environmental Monitoring
5. Socioeconomic Environmental Studies
6. Scientific and Technical Assessment Reports (STAR)
7. Interagency Energy-Environment Research and Development

This report has been assigned to the INTERAGENCY ENERGY-ENVIRONMENT RESEARCH AND DEVELOPMENT series. Reports in this series result from the effort funded under the 17-agency Federal Energy/Environment Research and Development Program. These studies relate to EPA's mission to protect the public health and welfare from adverse effects of pollutants associated with energy systems. The goal of the Program is to assure the rapid development of domestic energy supplies in an environmentally--compatible manner by providing the necessary environmental data and control technology. Investigations include analyses of the transport of energy-related pollutants and their health and ecological effects; assessments of, and development of, control technologies for energy systems; and integrated assessments of a wide range of energy-related environmental issues.

REVIEW NOTICE

This report has been reviewed by the participating Federal Agencies, and approved for publication. Approval does not signify that the contents necessarily reflect the views and policies of the Government, nor does mention of trade names or commercial products constitute endorsement or recommendation for use.

This document is available to the public through the National Technical Information Service, Springfield, Virginia 22161.

TECHNICAL REPORT DATA
(Please read Instructions on the reverse before completing)

1. REPORT NO. EPA-600/7-77-115	2.
3. RECIPIENT'S ACCESSION NO. PB273759	
4. TITLE AND SUBTITLE Nonwoven Fabric Filters for Particulate Removal in Respirable Dust Range	5. REPORT DATE October 1977
	6. PERFORMING ORGANIZATION CODE
7. AUTHOR(S) Bernard Miller, George Lamb, Peter Costanza, and Jeffrey Craig	8. PERFORMING ORGANIZATION REPORT NO.
9. PERFORMING ORGANIZATION NAME AND ADDRESS Textile Research Institute P.O. Box 625 Princeton, New Jersey 08540	10. PROGRAM ELEMENT NO. EHE624
	11. CONTRACT/GRANT NO. Grant R800042
12. SPONSORING AGENCY NAME AND ADDRESS EPA, Office of Research and Development Industrial Environmental Research Laboratory Research Triangle Park, NC 27711	13. TYPE OF REPORT AND PERIOD COVERED Final; 10/74-12-76
	14. SPONSORING AGENCY CODE EPA/600/13

15. SUPPLEMENTARY NOTES IERL-RTP project officer for this report is James H. Turner, Mail Drop 61, 919/541-2925.

16. ABSTRACT The report gives results of an extension of studies of the influences of fiber geometric properties on the ability of nonwoven fabrics to filter particles from gas streams to a wider range of geometric variables and to the measurement of capture efficiencies for particle sizes in the respirable range down to 0.024 micrometers. In addition to the light-weight (about 0.17 kg/sq m) fabrics studied earlier, commercial-weight (about 0.5 kg/sq m) fabrics were prepared from experimental fibers and evaluated in flat patch form. Some of these heavier fabrics were made into filter bags and tested in a laboratory baghouse equipped with automatic pulse-jet cleaning. Fibers with certain cross-sections (especially, trilobal) were found to increase flyash particle capture efficiency, especially in the submicron sizes, once a cake forms. The improvement occurs with no pressure drop increase. In comparing rough and smooth fibers, certain rough fibers appear to improve capture of the smallest particles after dust cake formation. Crimped fibers lead to better flyash filtration performance than uncrimped, but the crimp frequency has no noticeable effect. The capture efficiency increase accompanying a fiber diameter decrease follows different empirical relationships, depending on cake formation.

17. KEY WORDS AND DOCUMENT ANALYSIS

a. DESCRIPTORS	b. IDENTIFIERS/OPEN ENDED TERMS	c. COSATI Field/Group
Air Pollution	Air Pollution Control	13B
Dust	Stationary Sources	11G
Nonwoven Fabrics	Particulate	11E
Air Filters	Fabric Filters	11K
Filtration	Gas Streams	07D
	Geometric Properties	
	Baghouses	

18. DISTRIBUTION STATEMENT Unlimited	19. SECURITY CLASS (*This Report*) Unclassified	21. NO. OF PAGES 65
	20. SECURITY CLASS (*This page*) Unclassified	22. PRICE PCA04 - A01

EPA Form 2220-1 (9-73)

EPA-600/7-77-115
October 1977

NONWOVEN FABRIC FILTERS FOR PARTICULATE REMOVAL IN RESPIRABLE DUST RANGE

by

Bernard Miller, George Lamb,
Peter Costanza, and Jeffrey Craig

Textile Research Institute
P.O. Box 625
Princeton, New Jersey 08540

Grant No. R800042
Program Element No. EHE624

EPA Project Officer: James H. Turner

Industrial Environmental Research Laboratory
Office of Energy, Minerals, and Industry
Research Triangle Park, N.C. 27711

Prepared for

U.S. ENVIRONMENTAL PROTECTION AGENCY
Office of Research and Development
Washington, D.C. 20460

ia'

ABSTRACT

Studies of the influences of fiber geometric properties on the ability of nonwoven fabrics to filter particles from gas streams have been extended to a wider range of the geometric variables and to the measurement of capture efficiencies for particle sizes in the respirable range down to 0.024 μm. In addition to the light-weight ($\sim$0.17 kg/m^2) fabrics studied earlier, commercial-weight ($\sim$0.5 kg/m^2) fabrics have been prepared from experimental fibers and evaluated in flat patch form. Some of these heavier fabrics have been made into filter bags and tested in a laboratory baghouse equipped with automatic pulse-jet cleaning.

It was found that fibers having certain cross-sectional shapes (in particular, those with trilobal cross sections) can increase efficiency of capture of flyash particles, especially in the submicron size range, once a dust cake is formed. Such improvement occurs with no increase in pressure drop. When rough and smooth fibers are compared, certain rough fibers appear to improve capture of the smallest particles after dust cake formation. Crimped fibers lead to better flyash filtration performance than uncrimped fibers, but the frequency of the crimp does not have a noticeable influence. None of these improvements is observed unless an appreciable dust cake accumulates. A study of the effect of fiber linear density, at constant filter density and weight, has shown that the increase in capture efficiency accompanying a decrease in fiber diameter follows different empirical relationships depending on whether or not a cake forms. Differences between effects of fiber geometry in the presence and absence of a cake are taken to indicate that modifications of filtration performance resulting from changes in fiber geometry are largely due to the development of different cake structures.

In general, fiber geometrical factors affect the filtration behavior of commercial-weight fabrics in the same manner as they influence that of light-weight patch filters. Trials using commercial-weight fabric bags in the laboratory baghouse have confirmed that trilobal or rough fibers can produce practical filters with improved efficiencies at no cost to pressure drop.

This report is submitted in fulfillment of Grant No. R 800042-04 by Textile Research Institute under the sponsorship of the U.S. Environmental Protection Agency. This report covers a period from October 7, 1974 to October 6, 1976, and work was completed as of December 23, 1976.

CONTENTS

	Page
Abstract	ii
Figures	iv
Tables	vii
Abbreviations and Symbols	viii
Acknowledgments	ix
I. Introduction	1
II. Conclusions	2
III. Recommendations	4
IV. Apparatus	5
A. Patch Filter Apparatus	5
B. Aerosol Analysis	7
C. Pilot Baghouse	8
V. Experimental Results and Discussion	10
A. Effect of Linear Density on Capture Efficiency, Cake Resistance, and Air Permeability	10
B. Effect of Cross-sectional Shape	19
C. Effect of Surface Roughness	26
D. Effect of Crimp	33
E. Effect of Fabric Density	39
F. Results of Baghouse Trials	42
VI. References	51
VII. Conversion Table	52

FIGURES

Number		Page
1	Diagram of filtration apparatus	6
2	Particle size distributions of flyash measured by TSI and by AIR impactor	6
3	Baghouse layout	9
4	Characteristics of baghouse pump	9
5	Calibration curves for control of baghouse inlet concentration	9
6	Capture efficiency for three particle sizes vs. total length of fiber per unit volume of filter	12
7	Increase in effective particle diameter due to Brownian motion in 1/60 s	13
8	Dependence of capture efficiency on log of ratio of effective particle diameter (1/60 s) to mean interfiber spacing	13
9	Specific cake resistance (15th cycle) as a function of fiber diameter for PET and PP nonwoven fabrics of two weights	15
10	Penetration (15th cycle) as a function of fiber diameter for PET and PP nonwoven fabrics of two weights	15
11	Outlet concentration (10th cycle) of particles of several sizes as a function of fiber diameter for PP nonwoven fabrics	16
12	Dependence of Frazier air permeability on L_A, the total length of fiber per unit area, polypropylene fabrics	16
13	Capture efficiencies with no dust cake of fabrics made from round, trilobal, and pentalobal polyester fibers	20
14	Capture efficiencies with no dust cake of fabrics made from round and bilobal acrylic fibers	20
15	Ratio of outlet concentrations for bilobal acrylic fiber filters and for trilobal and pentalobal PET fiber filters to those for the corresponding round fiber filters	20

Figures (Cont)

Number		Page
16	Scanning electron micrographs of bilobal, trilobal, and pentalobal fiber cross sections	23
17	Scanning electron micrograph of bilobal acrylic fiber fabric showing distribution of short-axis orientation	25
18	Performance curves (C_0 vs. K) for trilobal and round fiber fabrics	25
19	Scanning electron micrographs of smooth and epitropic (surface-modified) fibers	27
20	Tenth-cycle efficiency distribution of nonconducting epitropic fiber filter, fabric density 0.11 g/cm^3	28
21	Tenth-cycle efficiency distribution of nonconducting epitropic fiber filter, fabric density 0.13 g/cm^3	28
22	Capture efficiency distributions for filtration of atmospheric dust through fabrics of commercial weight (492 g/m^2) measured without dust cake	30
23	Twentieth-cycle capture efficiency distribution for the fabrics in Figure 22 measured with a flyash aerosol and allowing cake to form	30
24	Capture efficiency distributions for polyester fabrics (16 oz/yd^2) measured without dust cake	32
25	Capture efficiency distributions for commercial-weight filters made of round smooth, round rough, and trilobal rough fibers, at the tenth cycle of filtering a flyash aerosol	32
26	Micrographs of rayon fibers	33
27	Capture efficiency distributions for rayon filters measured without dust cake	34
28	Capture efficiency distributions for rayon filters made with fibers at three levels of crimp: first cycle efficiencies with flyash aerosol	34
29	Comparison of capture efficiency for rayon filters made of fibers with 14.7 crimps per inch and 19.3 cpi with and without dust cake--atmospheric dust filtered through clean filter and through flyash cake	36
30	Capture efficiency distribution for regular and high crimp rayon filters at tenth cycle	36

Figures (Cont)

Number		Page
31	Outlet concentration distribution for four PET fabrics made of fibers with different crimp frequencies	38
32	Effect of fabric packing density on capture efficiency for various submicron particle sizes (PET-bonded PET fabrics)	40
33	Effect of fabric packing density on capture efficiency for various submicron particle sizes (Vinon-bonded PET fabrics)	40
34	Effect of packing density on clean fabric pressure drop for two PET fabrics: PET-bonded and Vinon-bonded	40
35	Effect of packing density on first-cycle efficiency for trilobal and round needled polyester fabrics	41
36	Effect of packing density on specific cake resistance for trilobal and round needled polyester fabrics	41
37	Initial and final pressure drops obtained with bags made of trilobal and round cross section fibers	44
38	Ratio of C_0 for a PET filter bag made of trilobal fibers to C_0 for a round-fiber bag as a function of particle diameter at several face velocities (table 12)	44
39	Efficiency of PET patch filter fabrics as a function of packing density at a face velocity of 30 mm/s	50
40	Efficiency of PET filter fabrics as a function of packing density at a face velocity of 60 mm/s	50
41	Cake resistance of PET filter fabrics as a function of packing density at the two face velocities, 30 and 60 mm/s	50

TABLES

Number		Page
1	SEM Measurements of Diameters of Flyash Particles Collected by "Air" Impactor	8
2	Fabric and Fiber Properties of Melt-blown Polypropylene Nonwovens	10
3	Fabric Construction of Vinyon-bonded PET and PP Nonwoven Filters	17
4	Filter Fabric Properties and Overall Filtration Performance of Conditioned Filters	21
5	Outlet Concentration for Conditioned Filters Made from Fibers of Different Cross-sectional Shape	22
6	Filtration Performance of Nonwoven Fabrics Made from Nonconducting Epitropic Fibers and Control PET Fibers	29
7	Properties of Commercial-weight Filter Samples Made from Polyester Fibers	31
8	Dependence of Pressure Drop Characteristics on Crimp Level for Rayon Fabrics	35
9	Properties of 14-oz Rayon Filters	37
10	Effect of Crimp Level in the Presence of a Cake	38
11	Specially Made Needled Polyester Fabrics	42
12	Outlet Concentrations for Trilobal and for Round Fiber Filter Bags at Various Face Velocities	43
13	Variations in Weight, Thickness, Density, and Standard Frazier Air Permeability of Bag Fabrics Listed in Table 11	45
14	Outlet Concentrations and Pressure Drops for Rough and Smooth-fiber Filter Bags at Various Face Velocities	47
15	Outlet Concentrations and Pressure Drops for Trilobal and for Round Fiber Filter Bags at Various Face Velocities	48

ABBREVIATIONS AND SYMBOLS

a	--fiber radius (μm)
α	--packing density
A.P.	--Frazier air permeability (ft/min)
C_o	--outlet concentration (g/m^3 or particles/m^3)
cpi	--crimps per inch
D_A	--aerodynamic particle diameter (μm)
D_M	--measured particle diameter (μm)
d	--effective particle diameter (μm)
E	--capture efficiency
1-E	--penetration
K	--specific cake resistance (N·s/kg·m)
L	--length of fiber per unit volume of fabric (m/cm^3)
L_A	--length of fiber per unit area of fabric (m/cm^2)
LD	--linear density (denier)
ΔP	--pressure drop ($\Delta P_f - \Delta P_i$) (mmH_2O)
ΔP_f	--final pressure drop before cleaning
ΔP_i	--initial pressure drop after cleaning
PET	--polyester
PP	--polypropylene
r	--particle radius (μm)
s	--mean interfiber spacing (μm)
TiO_2	--titanium dioxide

ACKNOWLEDGMENTS

The authors thank Dr. J. H. Turner of the Environmental Protection Agency for his advice and encouragement throughout the period of this research The authors also thank the E. I. du Pont de Nemours Co., Inc., ITT Rayonnier, and ICI Fibers, Ltd. (England) for supplying fibers, the Riegel Products Corporation for supplying meltblown nonwovens, and the J. P. Stevens Co. for making special needled fabrics.

SECTION I

INTRODUCTION

The modification of filtration performance of nonwoven fabrics by altering the geometric properties of constituent fibers was the subject of an earlier report [1]. That report, the fruit of a previous EPA grant, contained the findings that the diameter (or rather, linear density), cross-sectional shape, surface roughness, and crimp of the fibers had a significant effect on the capture efficiency and/or pressure drop characteristics of the fabric when it was used to filter a flyash aerosol. These results, however, were obtained in a rather limited program:

1. Only two levels of each geometric parameter were used.
2. The particle analyzer could measure only particles larger than 2.5 μm and therefore ignored a large portion of the respirable range.
3. The fabric samples were made to a weight of only ∿0.17 kg/m^2 (5 oz/yd^2) in order to magnify differences in performance. Only 100-mm patch filters were used.

The object of the present work was to expand the scope of the study from the above levels to:

1. A wider range of fiber geometric parameters.
2. Performance well into the respirable range for particles down to 0.1 μm or smaller.
3. A closer approximation to actual working conditions, that is with fabrics weighing ∿0.5 kg/m^2 (15 oz/yd^2) and, where possible, with fabric bags operating in a laboratory-scale baghouse.

These goals were largely achieved. Fabrics were prepared from a number of fibers having a range of the properties of interest, and pertinent results were obtained from filtration experiments made with them.

For particle size analysis, the Coulter Counter used in the previous study was replaced with a combination of a cascade impactor and an electrical aerosol analyzer. This combination allowed measurement of concentrations of particles from 0.024 to 10 μm in diameter.

In order to bring the results closer to practical conditions, a one-bag baghouse was constructed, and bags were fabricated from fabrics specially needled from various fibers. Because of the difficulty of obtaining special fibers in sufficiently large quantities and of having the fabrics made, only five such fabrics were obtained, but the results are of considerable interest.

SECTION II

CONCLUSIONS

The results of the present investigation extend to the submicron particle size range the conclusion of the previous study that proper selection of the geometric properties of the fibers composing a nonwoven filter can produce improvements in filtration efficiency without increasing pressure drop across the filter. The data suggest strongly that such improvements occur because fiber geometry determines the structure of the dust cake, which is the major filtering element of the combination of cake and fabric. Specifically:

1) Fiber cross-sectional shape influences the efficiency of filtration of flyash particles after a dust cake has formed, efficiency in the submicron particle size region increasing in the order: bilobal < round < pentalobal < trilobal. When a dilute aerosol, such as atmospheric dust, is filtered (so that negligible cake accumulates), filtration efficiency does not vary with cross-sectional shape. These improvements are achieved with no increase in pressure drop.

2) When the fiber surface is roughened by incorporation of TiO_2 particles, filtration efficiency is increased in the submicron particle size range with no change in pressure drop; again, there is no effect when a cake does not form. Improved efficiency is observed under certain conditions with fibers roughened by embedding other particles in the surface. There appears to be a need to quantify degree of surface roughness and investigate the effects of the composition of the material imparting the roughness.

3) Light-weight fabrics made of crimped fibers give somewhat better capture efficiencies over the entire size range than those made with uncrimped ones, but only when a flyash cake forms. The frequency of the crimp has no noticeable influence on efficiency or pressure drop at the fabric weights studied.

4) At constant fabric packing density and mass per unit area, a decrease in fiber diameter (linear density) increases both capture efficiency and pressure drop whether or not a cake is present. The variation of efficiency with fiber linear density, however, follows an altogether different empirical relationship when a dust cake forms than when none does, once again in agreement with the hypothesis that cake structure depends on fiber properties and in turn determines filtration behavior. Because pressure drop appears to approach limiting values as fiber diameter approaches zero,

it should be feasible to select fibers of low enough linear density to achieve the efficiency required for a particular application without too great an increase in pressure drop.

5) Increasing fabric weight from ∿0.17 to ∿0.5 kg/m^2 (commercial filter bag weight) did not eliminate the trends attributable to varying fiber geometrical properties.

6) The effects of cross-sectional shape and surface roughness observed with patch filters when a flyash cake forms generally remain the same for filtration through needled filter bags of commercial weight, tested for many cycles in a laboratory-scale baghouse.

Results obtained from baghouse experiments are presented and discussed in the last section of the report (Page 42). All results on preceding pages refer to experiments conducted with patch filters.

The rate of flow of air relative to the filter fabric is expressed in centimeters per second or feet per minute. The reader more familiar with a unit common to the filtration industry, the air-to-cloth ratio is reminded that the dimensions of this ratio are implicitly, feet per minute. Thus a face velocity of three feet per minute (or 1.5 cm/s) is equivalent to an air-to-cloth ratio of 3. The use of air-to-cloth ratio should in any case be discouraged since it may tend to be accepted as a dimensionless ratio, which would have the same value no matter what the system of units being used. In fact, the ratio has the dimension of velocity and will have a different value in different systems of units.

SECTION III

RECOMMENDATIONS

Results of the present study suggest that further work could be profitably undertaken in the following areas:

1. A microscopical study of the relationship between dust cake structure and filtration performance should be made with particular attention to the cake structure on fabrics found to give better performance. Understanding of the features associated with good performance should aid in the future design of filter fabrics.

2. Full-scale trials should be made using fabrics made of trilobal or rough-surface fibers to verify their commercial and environmental value.

3. Extension of the surface roughness study should include evaluation of filters made with fibers containing a wider range of TiO_2 levels. Since these are not commercially available, they would have to be specially made in small batches.

4. Extension of the study of cross-sectional shape effects should include evaluation of filters made with other multilobal fibers (especially tetralobal) and with fibers of different lobe depths.

SECTION IV

APPARATUS

A. PATCH FILTER APPARATUS

A typical experimental arrangement for work on gas filtration consists of three items: a device for generating the appropriate aerosol, a device for holding the filter and for conveying the aerosol to and through the filter, and an instrument for the determination of aerosol concentrations and particle size distributions.

There are problems associated with each component. The generation of aerosols by the dispersion of dust is attended by difficulties in feeding dust at a constant rate and in complete dispersion of the dust particles. The ideal arrangement of the ducts and filter holder must avoid turbulence, excessive loss of dust by deposition in the filter holder, and nonuniform velocity distribution. Analysis of the aerosol is most conveniently performed by means of one of a number of commercially available instruments; even then, some problems are created by the limitations of the instruments as to the range of sizes and concentrations that can be handled.

Our patch-filter apparatus is shown in Figure 1A. Most of the components were described in the previous report [1], but changes have been made in the dust feeder and dust removal systems. The feeder has a rotating drum with a slot cut in its cylindrical surface. As the slot passes under the hopper, it fills with dust. A vibrator keeps the dust flowing. When the slot reaches a position about 45° from the top center, it is emptied by a triangular scraper into a tee tube, in which an air jet disperses the dust into an aerosol. The aerosol enters an air chamber which serves the double function of smoothing the inlet concentration and catching the waste dust cake when the filter is cleaned.

A filtering cycle consists of five minutes of filtering at a face velocity of 6 cm/s (12 ft/min) and an inlet concentration of 6.7 g/m^3 followed by two minutes of reverse-air cleaning at 12 cm/s (32 ft/min). A sequence timer permits automatic filtering and cleaning through any number of cycles. Most measurements were made after the filter was conditioned for ten such cycles. Except where stated otherwise, the relative humidity was 40% and the ambient temperature 20°C. Cases in which the procedure deviated from the above are indicated in the text.

In some cases, it was necessary to examine the efficiency of a fabric in the absence of a dust cake. In these cases, ambient air was used as an aerosol. Ambient air contains concentrations of the order of 10^3-10^4 per cc of particles smaller than 0.5 μm. With such low concentration, a negligible amount of dust accumulated on the filter in the time taken for the measurements. This type of measurement is referred to in the text as being performed "without a dust cake" or "using atmospheric dust."

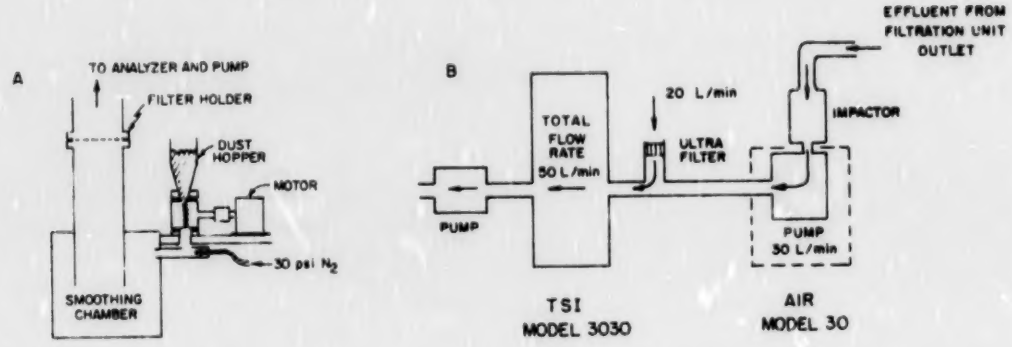

Figure 1 Diagram of filtration apparatus.

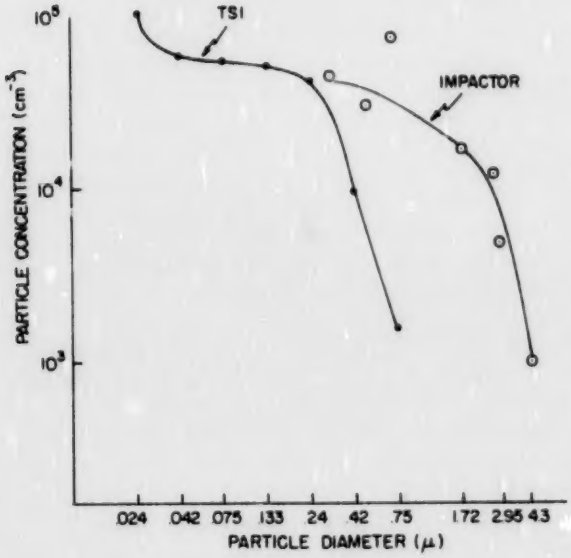

Figure 2 Particle size distributions of flyash measured by TSI and by AIR Impactor.

B. AEROSOL ANALYSIS

The aerosol analyzer is a combination in series of a Model 3030 electrical aerosol analyzer made by Thermo-Systems, Inc. (TSI) of St. Paul, Minn., and a Model 30 impactor made by AIR of Logan, Utah. Since the TSI unit operates at a flow rate of 50 ℓ/min and the AIR unit operates at 30 ℓ/min, an additional 20 ℓ/min of air is needed. This enters the system at a point between the two units after passing through an ultrafilter. (see Figure 1B).

The AIR impactor separates and collects particles from a gas stream by directing it at different velocities towards preweighed metal discs. This is accomplished by passing the gas through dish-like stages having increasingly small holes drilled in them. The higher the gas velocity, the smaller the particle that will hit the disc and stick to it. There are eight stages, designed to capture particles from 9 down to 0.275 μm in diameter. In practice, the last stage is eliminated, so that particles of 0.5-μm diameter are collected but all smaller particles pass into the TSI Model 3030. The TSI unit has a normal size range from 0.0042 to 0.75 μm, so that there is a region of overlap. Figure 2 shows particle size distribution results obtained with this combination. According to the manufacturers, the higher ranges of the TSI analyzer tend to give low readings. This appears to agree with the data in Figure 2, where the TSI readings at the two highest diameters deviate from the general trend of the combined impactor and TSI data. Accordingly, the two highest TSI ranges were discarded in favor of impactor readings.

At this time there is no available means for checking the accuracy of the TSI, but the impactor could be checked by scanning electron microscopy (SEM). Particles from the various collection stages of the impactor were photographed, diameters were measured from the photographs, and averages of about 30 observed particle diameters are listed in Table 1 along with the aerodynamic calibration values for each stage. A number of conclusions were drawn from these data:

1. The measured sizes are not too different from the nominal values, especially for the small diameters within the overlap region, where correspondence is very good.
2. The results show, however, that independent calibration (i.e., by SEM) is necessary. The impactor as supplied assigns an aerodynamic diameter to the particles captured by each stage. This is the diameter of most likely capture if the particles have unit density. The overall density of the flyash was measured and found to be 2.5 g/cm^3. However, if the nominal aerodynamic diameter (D_A) and the actual measured diameter (D_M) are known, the density at each stage is given by $\rho = (D_A/D_M)^2$ [2]. These calculated densities are included in Table 1 and are seen to vary from stage to stage. It must be remembered, therefore, that reported particle sizes cannot be readily translated into particle masses by assuming a common density.

3. The spread in the diameters of particles captured by each stage is fairly small, as shown by the calculated coefficients of variation listed in Table 1.

TABLE 1. SEM MEASUREMENTS OF DIAMETERS OF FLYASH PARTICLES COLLECTED BY "AIR" IMPACTOR

Nominal Aerodynamic Diameter, D_A (μm)	Measured Diameter, D_M (μm)	Coefficient of Variation, σ/D_M	Density $(D_A/D_M)^2$ (g/cm³)
9.0	5.1	0.3	3.1
5.7	4.0	0.2	2.0
3.4	2.7	0.2	1.6
1.9	1.6	0.2	1.4
1.0	1.0	0.3	1.0
0.5	0.5	0.3	1.0
0.3	0.3	0.2	1.0

C. PILOT BAGHOUSE

A diagram of the pilot baghouse is shown in Figure 3. A 122-cm long, 11.4-cm diameter bag is suspended in the center of a housing, whose inside dimensions are 30 cm x 38 cm x 150 cm. The average bag-to-wall distance is about one bag diameter. The aerosol is produced by feeding flyash from a BIF feeder into a 3-cm T junction, where it is dispersed by a jet of compressed air. The main air flow is produced by an air pump (vacuum cleaner) whose flow-pressure drop characteristics are shown in Figure 4. These characteristics naturally will vary from one pump to the next. They are shown here to illustrate the fact that vacuum cleaners, besides being inexpensive and readily available, are also adequate for this type of application. The bag is cleaned by the pulse jet method. The cleaning air is controlled by an ASCO valve which opens for about 0.1 s and is actuated by a timer switch.

It was observed that some of the flyash admitted to the baghouse never reached the bag but fell to the bottom of the chamber. Inlet concentration was determined by subtracting the amount on the bottom from the total fed in a given time, and dividing by the volume of air pumped in that time. Since the amount falling to the bottom varied slightly at different flow rates, the feeder settings necessary to give constant inlet concentrations were determined separately. The type of information obtained is plotted in Figure 5, and was used in the baghouse trials described in a later section.

All baghouse experiments were conducted at a relative humidity of 40% and a temperature of 20°C. Pulse-jet pressure was kept constant at 70 psi. Other experimental conditions, such as cycle time, inlet concentration, and face velocity, vary from trial to trial and are given in the text.

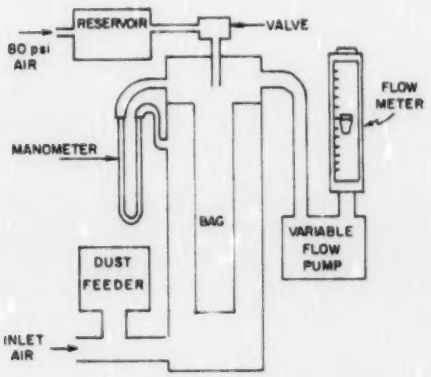

Figure 3 Baghouse layout.

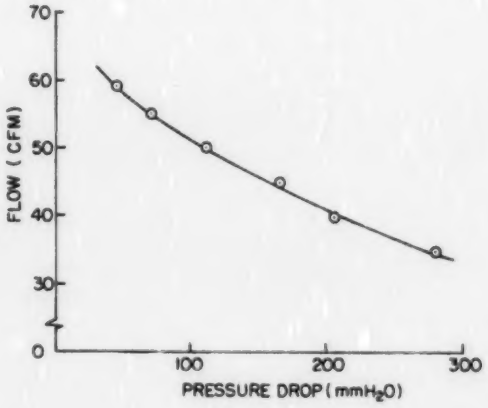

Figure 4 Characteristics of baghouse pump.

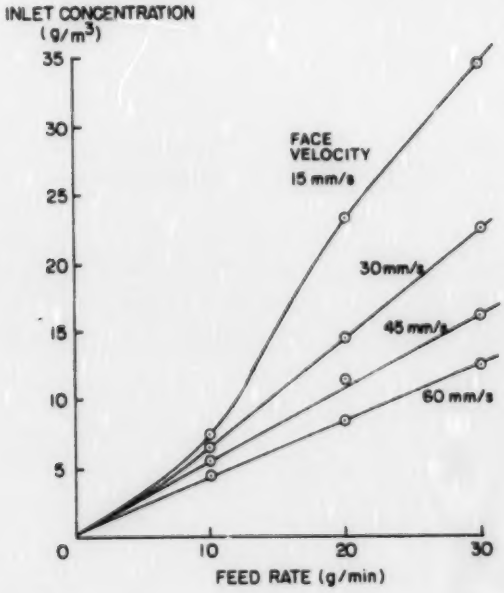

Figure 5 Calibration curves for control of baghouse inlet concentration.

SECTION V

EXPERIMENTAL RESULTS AND DISCUSSION

A. EFFECT OF LINEAR DENSITY ON CAPTURE EFFICIENCY, CAKE RESISTANCE, AND AIR PERMEABILITY

The previous study [1] was made with polyester fibers of 3 and 6-denier linear density (LD). It was found that higher LD gave lower efficiencies and lower pressure drop for equal weight filters. The range of LD was extended for the present study by the use of four polyester samples of 1.5, 2.25, 3.0 and 4.5 den, and polypropylene fibers of 1.8 and 3.0 den.

Extension of the LD range below 1.5 den was accomplished by using melt-blown polypropylene nonwovens obtained from Riegel Products Corporation. Melt-blowing is a technique whereby melted polymer from an extruder is acted upon by jets of air which attenuate the polymer into a mass of fine fibers. By varying melt temperature and the air jet pressure, some control over the fineness of the fibers can be achieved. These fibers are blown onto a belt where they form a sheet. Fourteen samples of this type of sheet made under a variety of the above conditions were supplied. Microscopical measurements showed that within each sheet there was a certain spread of fiber diameters - averages and 95% confidence limits were calculated and these are given in Table 2 along with corresponding LD and fabric weights, densities, and air permeabilities measured with a Frazier apparatus (A.P.). LD can be seen to range from 0.01 to 0.75 den.

TABLE 2. FABRIC AND FIBER PROPERTIES OF MELT-BLOWN POLYPROPYLENE NONWOVENS

Sample	Wt. (oz/yd^2)	Fabric density (g/cm^3)	Frazier A.P. (ft/min @ 0.5 in. H_2O)	ΔP_i (cm H_2O @ 12 ft/min)	Av. Fiber diam. (μm) ±95% C.L.	Av. Linear density (den)
1	2.84	0.14	160	0.45	2.49±0.46	0.046
2	3.07	0.08	91	0.50	1.74±0.64	0.026
3	2.78	0.07	298	0.20	3.26±0.93	0.084
4	2.98	0.12	797	0.10	8.36±3.97	0.678
5	2.90	0.04	192	0.30	1.25±0.18	0.011
6	2.53	0.07	1124	0.05	8.10±4.70	0.751
7	2.93	0.05	466	0.15	3.18±2.20	0.130
8	2.69	0.04	231	0.25	2.15±0.72	0.039
9	2.78	0.05	252	0.25	2.85±1.42	0.081
10	2.98	0.04	198	0.40	1.47±0.46	0.018
11	2.64	0.08	416	0.15	5.69±2.10	0.279
12	2.70	0.05	199	0.30	2.52±0.96	0.055
13	2.70	0.12	141	0.40	1.92±0.61	0.032
14	2.78	0 08	118	0.45	1.59±0.50	0.021

A first experiment used these light-weight melt-blown fabrics and two polypropylene fabrics made from the 1.8-den and the 3.0-den fibers bonded together with Vinyon and controlled to the same weight and density as some of the melt-blown webs (3 oz/yd^2 and 0.12 g/cm^3, respectively). Measurements were made of submicron particle filtration efficiency using atmospheric dust with no cake. Results of these measurements are plotted in Figure 6 vs. the log of total fiber length per unit volume. This quantity is inversely proportional to the fiber linear density if the fabric packing density (ratio of fiber volume to fabric volume) is kept constant. It can be seen that efficiency increases linearly with the log of the relative total length of fiber. The slope of the line is approximately the same for 0.024, 0.075, and 0.24-μm particles There appears to be no effect of fabric packing density, since four of the melt-blown samples are lower in density than the others (0.07 - 0.08 g/cm^3) but fall on the same straight lines.

Interpretation of the above results involves comparison of interfiber distances in the fabric with the effective dimensions of small particles under the action of Brownian motion. Brownian motion results in a net displacement of a particle in a given time interval. The average displacement $\bar{x}$ in a given direction during time t is given by [3]

$$(\bar{x})^2 = (kT)\ (t/3\pi\eta r)\ (1 + 0.9\ \ell/r), \qquad (1)$$

where η is the viscosity of air,
ℓ, the mean free path in air,
r, the particle radius,
k, Boltzmann's constant,
T, the absolute temperature, and the term $(1 + 0.9\ \ell/r)$ is known as the Cunningham correction. The importance of this relationship is illustrated in Figure 7 which plots effective diameter ($d = 2r + \bar{x}$) as a function of the actual particle diameter. Equation (1) predicts that the effective diameters of particles increase with time, so that for a particular filter they will depend on the residence time in the filter. In Figure 7 effective diameters are plotted for the case where the face velocity is 6 cm/s and the fabric is 1-mm thick, giving a residence time (t) of 1/60 s.

The mean interfiber distance (s) may be calculated as follows: If the packing density (volume of fiber/volume of fabric) is α and the fiber radius is a, the total length (L) of fiber per unit volume of fabric is $\alpha/\pi a^2$. Assuming that the fibers are all oriented in the plane of the fabric and that half are parallel to the x direction and half to the y direction, the number of fibers passing through a y-z face of a unit cube would be $\alpha/2\pi a^2$. If the fibers are arranged in a square array, the number of fibers in a side of a unit square is $\sqrt{\alpha/2\pi a^2}$. The mean distance (s) between fibers is then $\sqrt{2\pi a^2/\alpha}$.

Figure 8 is a plot of capture efficiency (from Figure 6) vs. ln d/s for particles with actual diameters from 0.024 to 0.24 μm

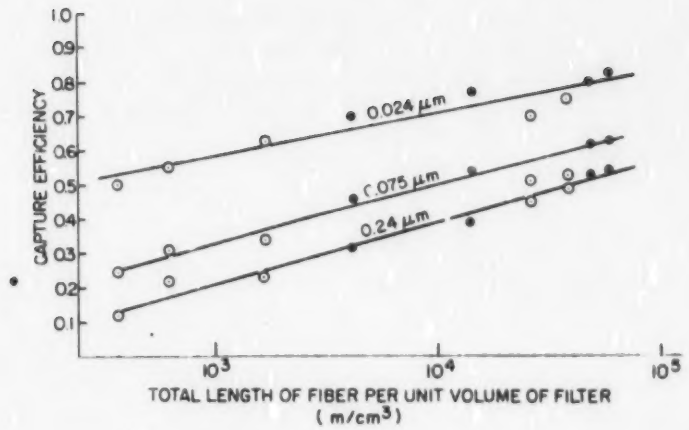

Figure 6 Capture efficiency for three particle sizes vs. total length of fiber per unit volume of filter. PP 3 oz/yd^2, packing density 0.12 - 0.14 (∘) and 0.07 - 0.08 (•). No dust cake.

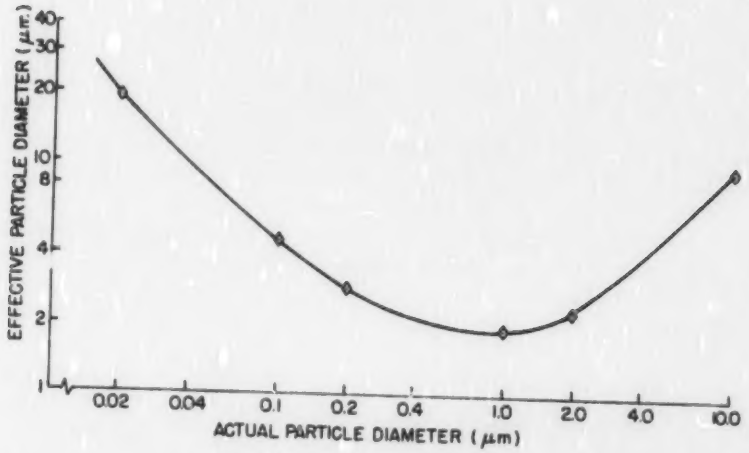

Figure 7 Increase in effective particle diameter due to Brownian motion in 1/60 s.

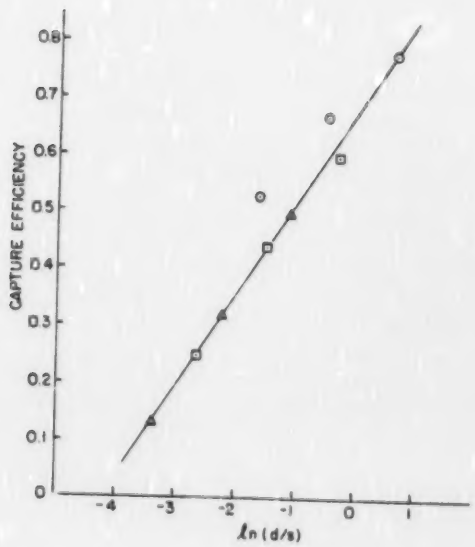

Figure 8 Dependence of capture efficiency on log of ratio of effective particle diameter (1/60 s) to mean interfiber spacing, for particles of actual diameter 0.024 μm (o), 0.075 μm (●), and 0.24 μm (Δ).

and for fabrics made of fibers with radii 1 to 10 μm. All points are seen to fall close to a common line. The empirical relationship is

$$E = 0.17 \ln d/s + 0.68, \quad (2)$$

although the line is not expected to remain straight for very high or very low efficiencies, since it must approach efficiencies of zero or one asymptotically. Assuming that the line was straight over the whole efficiency range would be a reasonable approximation, since an efficiency of one would occur when d/s was 4.5 (i.e., when the effective particle diameter was 4.5 times the mean pore size), and zero capture when d/s was 0.011.

To examine the effect of fiber diameter on the filtration of a flyash aerosol, four of the polypropylene fabrics were used in patch-filter experiments in which a cake was allowed to form. The results in Figures 9 (lower curve) and 10 (upper curve) show that, as fiber diameter decreases, specific cake resistance and efficiency tend to limiting values.

The curves in Figure 11 which plot outlet concentration for several particle sizes vs. fiber diameter suggest a relationship of the type

$$\ln (1-E) \propto s, \quad (3)$$

since the mean interfiber spacing (s) is proportional to the fiber diameter and the penetration (1-E) is proportional to the outlet concentration. This contrasts with the findings for clean filters where the relationship was found to be of the form (Figure 8, equation 2):

$$(1-E) \propto 0.17 \ln s/d, \quad (4)$$

or, for one particle size, $(1-E) \propto \ln s$.

The difference is clearly due to the filtering characteristics of the dust cake, but no analytical explanation is available at this time.

A second experiment with commercial-weight filters (Table 3) used four polyester (PET) and two polypropylene (PP) fibers, bonded with 10% Vinyon, a low melting point fiber. Table 3 shows that the PET and PP filters were kept at constant packing density. The density of PP is 0.98 and that of PET is 1.38. In order to obtain fabrics of the two polymers having equal volumes of fiber per unit fabric area, the unit masses of fiber were made inversely proportional to the fiber density. The results are plotted in Figure 9 (upper curve) and Figure 10 (lower curve).

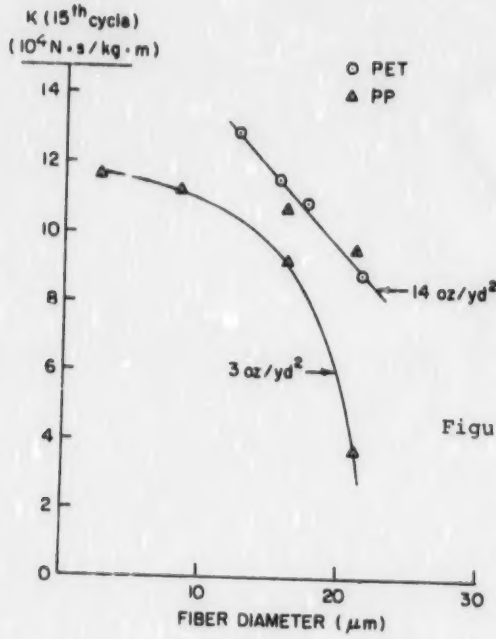

Figure 9 Specific cake resistance (15th cycle) as a function of fiber diameter for PET and PP nonwoven fabrics of two weights.

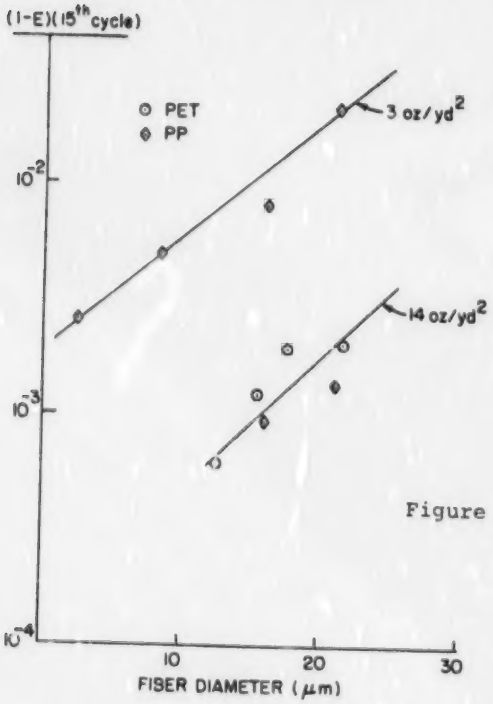

Figure 10 Penetration (15th cycle) as a function of fiber diameter for PET and PP nonwoven fabrics of two weights.

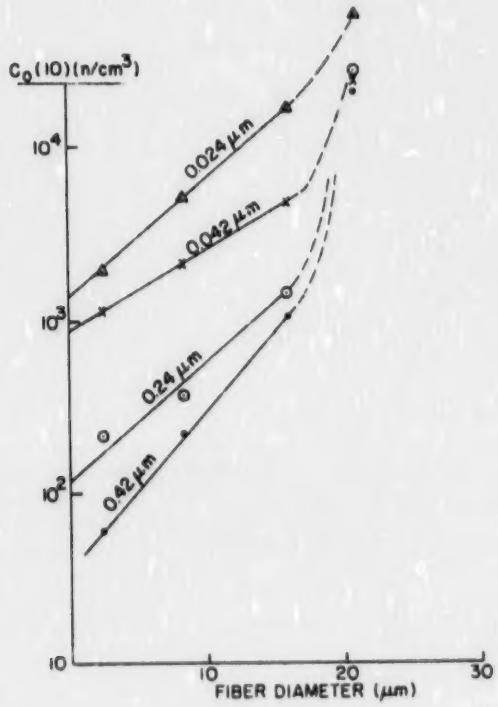

Figure 11 Outlet concentration (10th cycle) of particles of several sizes as a function of fiber diameter for PP nonwoven fabrics (14 oz/yd^2).

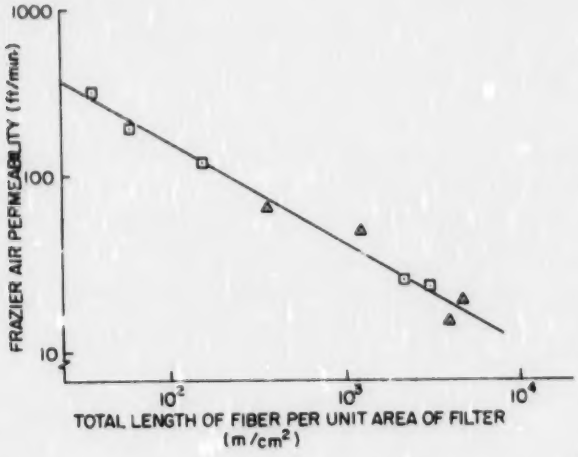

Figure 12 Dependence of Frazier air permeability on L_A, the total length of fiber per unit area. Polypropylene fabrics with packing density 0.12 - 0.14 (□) and 0.07 - 0.08 (Δ).

TABLE 3. FABRIC CONSTRUCTION OF VINYON-BONDED PET AND PP NONWOVEN FILTERS

Linear density (tex)	(denier)	Fabric Wt. (oz/yd^2)	Fabric density (g/cm^3)	Packing density	Fiber diameter (μm)
0.167	1.5	13.65	0.193	0.140	12.5
0.25	2.25	13.60	0.192	0.139	PET 15.5
0.333	3.0	13.58	0.188	0.136	17.5
0.50	4.5	13.57	0.190	0.138	21.5
0.20	1.8	9.97	0.138	0.141	PP 16
0.333	3.0	9.99	0.135	0.138	21

The following conditions were kept constant:

Face velocity:	61 mm/s (12 ft/min)
Dust loading:	6.7 g/m^3
Volumetric flow rate:	497 cm^3/s (1.05 ft^3/min)
Area of filter:	81.07 cm^2 (0.0873 ft^2)
Relative humidity:	40% ± 2%

It can be seen that the log of fifteenth-cycle penetration [(1-E)(15)] increases with fiber diameter. Results for PP and PET fall on the same curve. Since PET fibers of less than 1.5 den were not available, the curve for the heavier fabrics must be assumed, tentatively, to tend to a limiting value for zero denier as does the upper curve for melt-blown PP. It may also be assumed that there will be different curves corresponding to different binder contents which produce different packing densities. The results suggest that as fiber diameter decreases, cake resistance and efficiency tend to a value largely determined by the structure of the cake. The density of a fabric as a function of distance from its mid-plane drops more or less abruptly as the fabric surface is approached. The boundary layer within which the density falls from the maximum to zero may be assumed to vary in thickness with the fabric density, being greatest for low density fabrics, and almost zero for very compact fabrics. The cake formed on a boundary layer corresponding to a certain density may be expected to give efficiencies and cake resistances characteristic of that boundary and tending to limiting values as LD tends to zero. In turn, as fabric density increases, these limiting values will tend to a value corresponding to a cake unaffected by interference from the fabric structure. Such a cake might ideally be formed by deposition on a perfectly permeable flat surface. It is possible that as LD decreases and fabric density increases, the surface topography of the fabric approaches more nearly a plane on which such an ideal cake might be formed. A more complete description of the manner in which structural features account for differences in cake resistance must await further studies, both experimental and theoretical.

In conclusion, a decrease in fiber linear density at constant fabric weight results in an increase in both capture efficiency and pressure drop. The dependence of these responses on linear density is different in the cases where a very dilute aerosol is

filtered from those where the aerosol is concentrated enough to form a dust cake. In the former case, both efficiency and pressure drop characteristics show a linear dependence on the log of the linear density (or its inverse, the total length of fiber per unit area of fabric). In the case where a dust cake is formed, specific cake resistance, when plotted against the log of linear density, shows nonlinear relationships which appear to tend toward limiting values.

With regard to practical application, the fact that a variation in the linear density involves a trade-off between the two responses means that there will probably be an optimum linear density for each specific application. The value of the above findings may, however, lie less in their use as guides for the selection of fabric construction parameters than in their role in clarifying the mechanisms of filtration.

It would be instructive to be able to relate linear density and air permeability (A.P.), the air velocity required to give a pressure drop of 0.5 in. H_2O, a measure of the resistance of a fabric to flow. Air permeabilities measured with a Frazier apparatus on the same samples are plotted in Figure 12 as a function of L_A, the length of fiber per unit area of fabric. The empirical relationship is very nearly of the form

$$\text{A.P.} \propto L_A^{-\frac{1}{2}} \propto (LD)^{\frac{1}{2}} \propto 2a. \tag{5}$$

Fitting this type of relationship to a model is difficult. According to Spielman and Goren [4], Stokes' equations do not yield a solution for flow past an isolated cylinder, and analysis of flow through a mat of cylinders is best accomplished beginning with Brinkman's model [5], which leads to

$$\nabla P = \mu \nabla^2 \vec{u} - \mu k \cdot \vec{u}. \tag{6}$$

That is to say, the fluid flowing around an obstacle in a collection of obstacles experiences viscous forces given by the first term and damping forces due to the proximity of the other obstacles, given by the second term, where p is the average pressure field, $\vec{u}$ the average velocity field, μ the fluid viscosity, and k a tensor giving the damping coefficients.

Spielman's treatment does not readily yield a relationship between pressure drop and fiber diameter. Given the complexity of the derivation, it may be sufficient to note the empirical relationship, remembering that the pressure drop due to the filter fabric alone is only a fraction of what it is with an accumulated dust cake. A more fruitful study would be the dependence of pressure drop on various cake formations, such as may be variously formed on fabrics made from different fibers or under the influence of electric fields.

B. EFFECT OF CROSS-SECTIONAL SHAPE

This part of the study was hampered somewhat by the difficulty in obtaining a series of fibers which would differ only in their cross-sectional shape. Although an ample choice appears to be available, it is not enough to select samples to represent different cross sections. If they also differ in some other physical property, this difference will have an unknown effect on the measured responses. For this reason, only five fiber types were used: three polyester fibers, round, trilobal, and pentalobal in cross section, and two acrylic fibers, round and bilobal. Fabrics were made with each of these and their filtration performance measured with and without a dust cake.

The results in Figure 13 (for the PET fabrics) and in Figure 14 (for the acrylic fabrics) show that cross-sectional shape has no measurable effect on submicron capture efficiency when no cake is present. Nonround cross-sectional shapes are assumed to reduce interfiber gaps (as opposed to center-to-center distances) since projected fiber diameters are increased. For example, a change from round to trilobal cross section decreases the interfiber gaps for the fabrics in Figure 13 from 41.8 to 38.3 μm. These values were obtained from SEM micrographs. Equation (4) indicates that this change should result in an increase in efficiency of only 1.8% for all particle sizes. This is too small to detect, as is confirmed in Figure 13. The same argument applies to the comparison of round and bilobal fibers which have very similar efficiencies as seen in Figure 14.

At a face velocity of 0.061 m/s all clean filters exhibited about the same pressure drop: the set of three polyester samples produced about 2 mm H_2O, and the two acrylic samples about 3 mm H_2O. The Frazier air permeability is more sensitive, and these data are included in Table 4 and reveal differences between the samples. It can be seen that round fibers resist air flow less than pentalobal fibers, which are less resistant than trilobal fibers. In the acrylic fabric comparison, round fibers resist air flow less than bilobal fibers.

In the evaluation of the fabrics with a flyash aerosol, i.e., in the presence of a dust cake, the polyester samples were conditioned for nine filtering-cleaning cycles on the patch filter apparatus. Dust loading was 6 g/m^3 at 0.061 m/s face velocity for five minutes. Measurements of efficiency and pressure drop characteristics were then made during the next seven cycles. Table 4 gives average values for specific cake resistance and overall penetration. It can be seen that no significant differences in specific cake resistance are found.

Differences in efficiency, however, are somewhat greater in the presence of a cake then without it (Figures 13 and 14), as can be seen in Figure 15 and Table 4. This tends to indicate that the formation of a cake is affected by interfiber spacing or by some other effect associated with differences in cross-sectional shape.

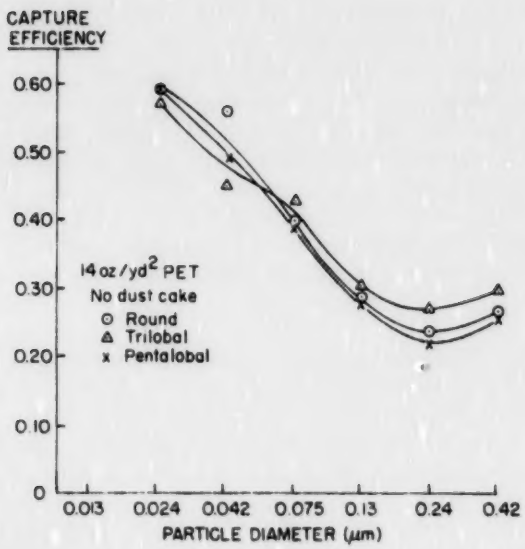

Figure 13

Capture efficiencies with no dust cake of fabrics made from round, trilobal, and pentalobal polyester fibers.

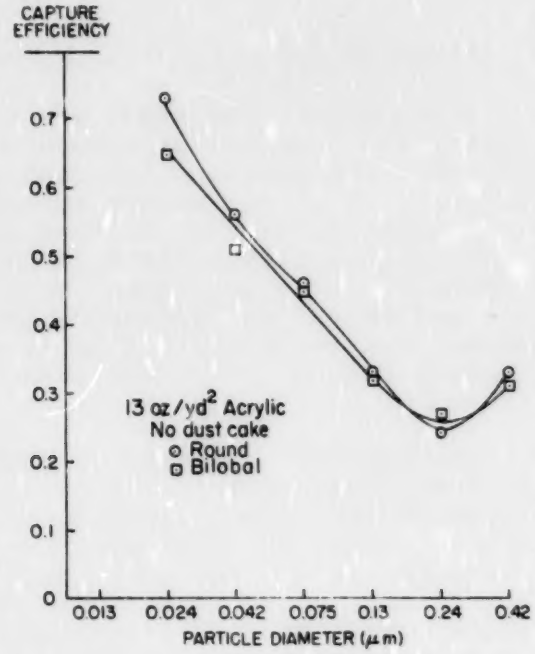

Figure 14

Capture efficiencies with no dust cake of fabrics made from round and bilobal acrylic fibers.

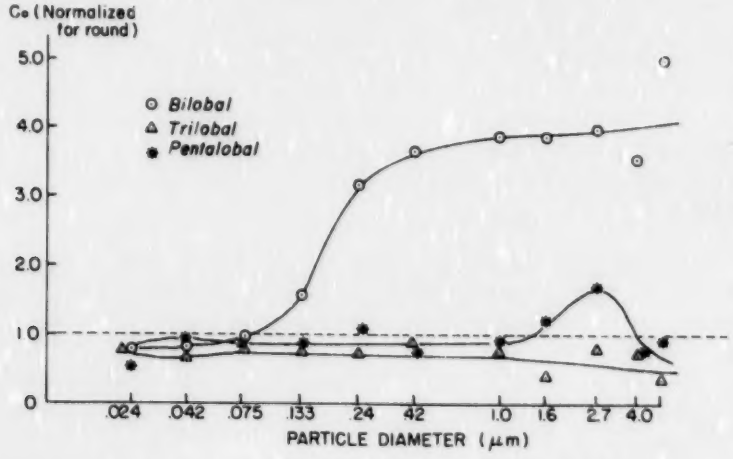

Figure 15 Ratio of outlet concentrations for bilobal acrylic fiber filters and for trilobal and pentalobal PET fiber filters to those for the corresponding round fiber filters.

The formation of a cake depends on bridging, and a reduction in fiber spacing should not only increase impact probability, but also allow more rapid bridge formation. Since the bridge is shorter, it is more stable and resists collapse, and greater capture efficiency is therefore observed.

TABLE 4. FILTER FABRIC PROPERTIES AND OVERALL FILTRATION PERFORMANCE OF CONDITIONED FILTERS

(Face Velocity 0.061 m/s) Inlet Concentration 6.7 g/m^3 Mercer Flyash)

	Polyester			Acrylic	
	Round	Trilobal	Pentalobal	Round	Bilobal
Wt. (kg/m^2)	0.487	0.487	0.479	0.453	0.463
Wt. (oz/yd^2)	14.3	14.3	14.1	13.3	13.6
Fabric density (g/cm^3)	0.192	0.197	0.196	0.198	0.194
Packing density	0.139	0.142	0.142	0.168	0.164
Fiber linear density (den)	3.04	3.20	3.19	3.31	3.29
Specific cake resistance, K (10^6N·s/kg·m)	11.2	11.1	10.2	10.2	10.8
Penetration (%)	0.073	0.043	0.078	0.019	0.077
Air permeability (ft/min)	65.5	49.5	58.2	43.3	35.1
Average interfiber gap (μm)	41.8	38.3	40.4	42.2	33.28* 49.50**

* All fibers oriented with min. proj. diam. normal to air flow.

** All fibers oriented with max. proj. diam. normal to air flow.

Measurements were also made of outlet concentration C_o (Table 5) and are shown in Figure 15, expressed as the ratio of C_o for the non-round fiber to C_o for the corresponding control round fiber. Trilobal PET fibers appear to be slightly more efficient than pentalobal over most of the range of particle sizes. Pentalobal fibers are more efficient than round in the submicron region, and are about equal on the average to round fibers in the region above 1 μm.

TABLE 5. OUTLET CONCENTRATION FOR CONDITIONED FILTERS MADE FROM FIBERS OF DIFFERENT CROSS-SECTIONAL SHAPE

(Overall inlet concentration is kept constant at 6.7 g/m^3)

Particle size (μm)	Outlet concentration (particles/cm^3 x 10^3)				
	Polyester*			Acrylic**	
	Round	Trilobal	Pentalobal	Round	Bilobal
0.024	2.98	2.45	1.67	2.31	1.81
0.042	1.35	0.94	1.28	0.70	0.61
0.075	1.53	1.22	1.30	1.16	1.13
0.133	1.35	1.07	1.12	0.83	1.31
0.24	0.43	0.33	0.47	0.16	0.51
0.42	0.31	0.27	0.24	0.11	0.40
1.0	1.15	0.89	1.07	0.26	1.02
1.6	0.25	0.11	0.41	0.031	0.12
2.7	0.016	0.013	0.026	0.0129	0.0518
4.0	0.004	0.003	0.003	0.0011	0.0039
5.1	0.00045	0.000	0.00042	0.0003	0.0019

* Average values for 10th through 13th cycle.

** Values for 11th cycle.

The failure of the pentalobal fibers to give an improvement in performance comparable to that found with trilobal fibers is explained by Figure 16. This shows cross sections of the fibers used, and it is evident that the lobes in the pentalobal fibers are rather shallow. It is clear, therefore, that a simple description of the cross-sectional shape such as trilobal, pentalobal, etc., is sufficient only for exploratory purposes. For a more exhaustive study, the influence of the depth of the lobes should be taken into account.

The bilobal and round acrylic fiber samples were evaluated in a similar manner. Samples were conditioned for ten cycles and measured on the 11th for specific cake resistance, overall penetration, and outlet concentration for the full range of particle sizes. Data are given in Table 4. Specific cake resistance is only slightly higher for bilobal than for round, but overall penetration is four times greater for the bilobal fibers. Outlet concentrations are considerably higher for bilobal fibers for most particle sizes (see Figure 15).

For nonwovens of equal weight and volume, and equal total length of fibers, the average distance between fiber centers is independent of shape, but if a given shape has a greater projected diameter, the gap between fibers will be smaller. Calculated average interfiber gaps are given in Table 4. Since the projected area of a bilobal fiber is more strongly dependent on orientation than the others, values are given for both extreme cases of orientation for these fibers.

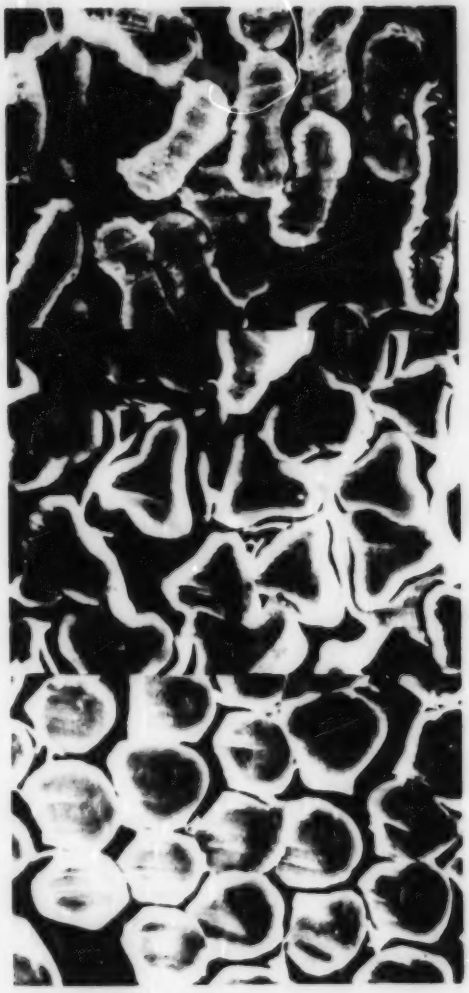

Figure 16 Scanning electron micrographs of bilobal, trilobal, and pentalobal fiber cross sections.

The effect on penetration due to a change in cross-sectional shape from round to trilobal may be compared with the corresponding change due to a decrease in fiber diameter in fabrics made of round fibers. Table 4 indicates that the gap between fibers in a trilobal fabric of packing density 0.14 is 38.3 μm. The corresponding distance in a "round" fabric of the same packing density is 41.8 μm. In fabrics made of round fibers, the mean center-to-center spacing (s) is given by

$$s = \sqrt{2\pi a^2/\alpha} ,$$

remembering that a is the fiber radius and α the packing density. The interfiber gap is therefore

$$s-2a = \sqrt{2\pi a^2/\alpha} -2a.$$

Solving this equation for a, with (s-2a) equal to 38.3 and 41.8 μm, gives fiber diameters (2a) of 16.2 and 17.8 μm, respectively. The penetrations of filters made of round fibers with these diameters can be found from the lower curve of Figure 10 and are .0011 and .00137. We see, therefore, that a reduction in gap due to the increase in the total length of round fiber leads to a reduction in penetration of 20%, but an equal reduction in gap obtained by altering cross-sectional shape at constant fiber length leads to a reduction in penetration (Table 4) from .00073 to .00043, or 40%. This suggests that easier bridging by a reduction in the interfiber gap is not the only explanation of the improved efficiency given by trilobal fibers. It is possible that better single fiber efficiency and better adhesion efficiency may also contribute.

For bilobal fibers the apparent lack of correlation between average pore area and outlet concentration may be a result of wider fluctuations of projected area with orientation. Random orientation of bilobal fibers in the structure will result in a distribution of pore areas which is wider than in the case of round fibers. Consequently, there will be a certain number of larger pores in the bilobal filter through which seepage may occur. Scanning electron micrographs (Figure 17) verify the random orientation of cross-sectional shape.

In summary, fibers with modified cross sections whose projected diameters are greater than the projected diameters of round fibers of equal LD will increase capture efficiency over the entire range of particle sizes. The effect is due not only to the reduction in interfiber spacing, which would also result from a decrease in linear density at constant fabric weight and packing densities. This is illustrated in Figure 18 which compares performance curves for round and trilobal fiber fabrics previously reported [1]. In such a plot improved performance corresponds to closer proximity of the curve to the origin. It is seen that a change from round to trilobal fibers moves the performance curve to a better position.

Figure 17 Scanning electron micrograph of bilobal acrylic fiber fabric showing distribution of short-axis orientation.

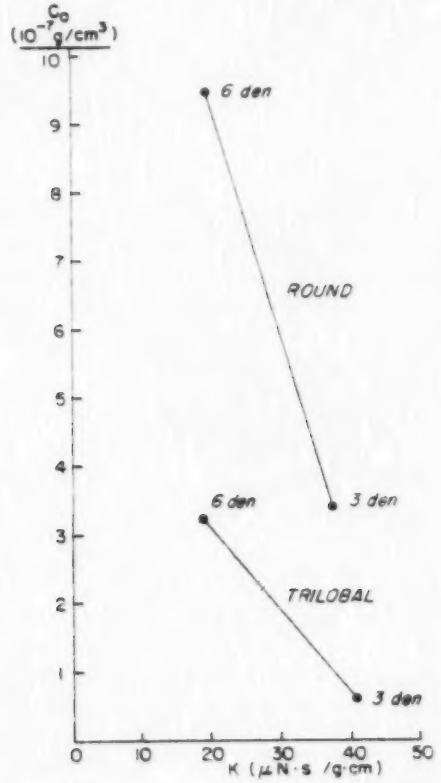

Figure 18 Performance curves (C_0 vs. K) for trilobal and round fiber fabrics. The ideal curve would be a single point at the origin. Better performance of trilobal fibers is shown by greater proximity of their curve to the origin.

A further experiment was performed to confirm the differences in performance between fabrics made with round vs. trilobal fibers and rough vs. smooth fibers when the fabrics were of commercial weight ($\sim$0.5 kg/m^2). Since this trial also involved comparisons of the effect of surface roughness, the account is to be found in the following section.

C. EFFECT OF SURFACE ROUGHNESS

The property of surface roughness is probably the most troublesome to study, since it is hard both to control and to express quantitatively. The previous study of surface roughness effects [1] employed polyester fibers with two levels of roughness produced by incorporation of 0.1% and 2.0% TiO_2. These fibers were also used in expanded roughness studies, but the search for other rough-surfaced fibers that would provide a wider range of the property yielded only one more: a nonconductive epitropic (i.e., surface-modified) fiber, shown in Figure 19.

These epitropic fibers consist of a core of polyester and an outer sheath of low melting polyester into which are embedded particles smaller than 5 μm. At first, the only samples available for study had carbon black particles embedded in their surfaces [6]. Although these fibers possessed a considerably higher degree of surface roughness, their primary application is in the reduction of static charge buildup in textile materials. Instead of enhancing filtration efficiency in the small particle region, samples made from these fibers were found to be less efficient than comparable samples made with smooth fibers. An explanation of this anomalous result seemed to lie in the electrical conductivity of the carbon black. If there is a tendency for charge buildup on a filter while it is operating, such charges would be leaked away by conducting fibers. This would nullify any electrostatic aggregation of particles with its associated increase in collection efficiency. Presumably this effect was greater than any improvement due to surface roughness.

Fortunately, the manufacturer (ICI) also produces experimental quantities of epitropic fiber with nonconducting particles embedded in the surface, though the nature of these particles has not been disclosed. Some of these fibers were obtained from ICI along with a control sample of untreated polyester for comparison. Lightweight filters were then prepared from cross-laid card webs using 10% Vinyon low-melting fiber as binder. Epitropic samples and control samples of two fabric densities, 0.11 and 0.13 g/cm^3, were compared for efficiency and drag characteristics at the tenth cycle. The results are given in Table 6 and Figures 20 and 21.

In comparing efficiencies, the most significant differences can be seen in the efficiency distribution curves. Although overall efficiencies, E(10), show that the epitropic samples are not

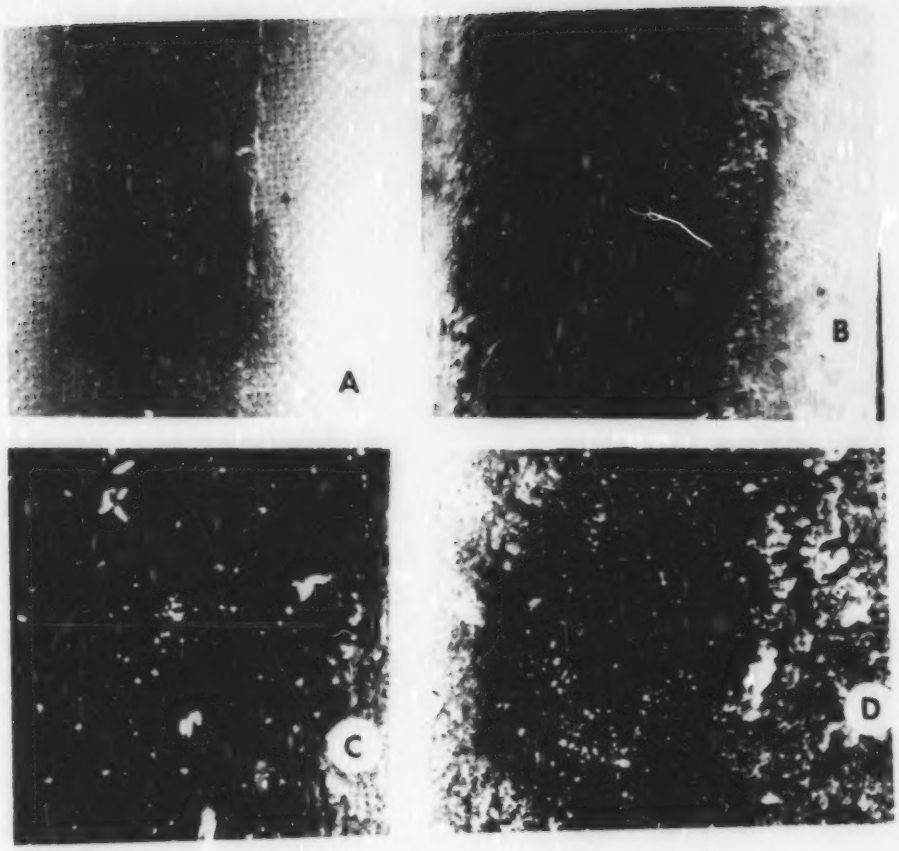

Figure 19 Scanning electron micrographs of smooth and epitropic (surface-modified) fibers.

A. Control 2000X B. Epitropic 2000X
C. Control 6000X D. Epitropic 6000X

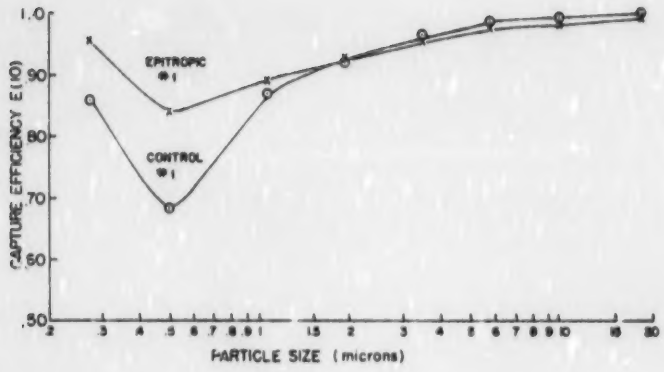

Figure 20 Tenth-cycle efficiency distribution of non-conducting epitropic fiber filter. Fabric weight 170 g/m^2 (5 oz/yd^2); density 0.11 g/cm^3.

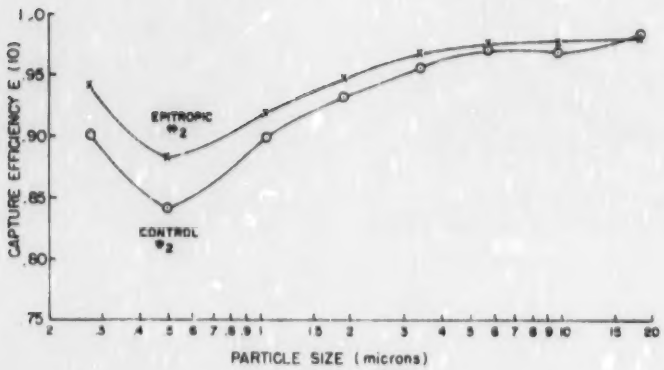

Figure 21 Tenth-cycle efficiency distribution of non-conducting epitropic fiber filter. Fabric weight 170 g/m^2 (5 oz/yd^2); density 0.13 g/cm^3.

significantly better than the control samples, differences are evident in the region below 2 μm. It is clear that the epitropic samples capture these small particles better than the control samples. These results thus tend to support the explanation of the ineffectiveness of conducting epitropic fibers, as well as the initial findings of increased efficiency for capture of small particles using TiO_2-roughened fibers.

Differences in drag characteristics (Table 6) seem to be dependent on fabric density. The epitropic filter has appreciably higher drag characteristics than the control filter, but the difference is smaller for the denser samples.

TABLE 6. FILTRATION PERFORMANCE OF NONWOVEN FABRICS MADE FROM NONCONDUCTING EPITROPIC FIBERS AND CONTROL PET FIBERS

	Epitropic	Control	Epitropic	Control	Epitropic	Control
Wt. (g/m^2)	163	170	173	173	492	492
Density (g/cm^3)	0.11	0.11	0.13	0.13	0.11	0.11
Efficiency (%)	97.3	98.0	97.1	96.5	99.5	99.5
ΔP (mmH_2O)	17	10	27	25	38	38
$K(10^3$ N·s/kg·m)	10.0	6.5	19.7	18.8	92.3	93.2

The effect of fiber surface roughness was further examined by forming fabrics of commercial weight (492 g/m^2 or 14.5 oz/yd^2, density 0.11 g/cm^3) from the nonconducting epitropic fibers and from the control fibers. The performance without dust cake using ambient air dust was measured first. The results in Figure 22 show again that the epitropic filter is more efficient than the control in the submicron range. In contrast, when a flyash aerosol is filtered and performance is evaluated after 20 filtering cycles when a dust cake has formed, the results shown in the last two columns of Table 6 and in Figure 23 are obtained. There are no significant differences between the filter made of epitropic fibers and the control for these conditions.

Examination of the effect of surface roughness was continued using TiO_2-roughened fibers as part of a preliminary trial for the preparation of fabrics for use with the laboratory baghouse. Commercial-weight (16 oz/yd^2) samples were made from the following PET fibers:

3-den, 1.5-in., round, smooth (0.1% TiO_2), 11 crimps/in.
3-den, 1.5-in., round, rough (2.0% TiO_2), 11 crimps/in.
3-den, 1.5-in., trilobal, rough (2.0% TiO_2), 11 crimps/in.

Fabric properties are listed in Table 7, which also lists pressure drops and specific cake resistances for the three samples. Very small differences were found between them, confirming previous findings [1].

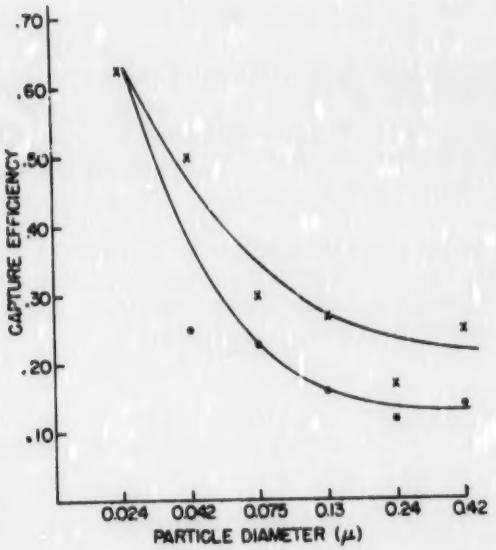

Figure 22 Capture efficiency distributions for filtration of atmospheric dust through fabrics of commercial weight (492 g/m^2) measured without dust cake. Fabrics made of nonconductive epitropic fibers (x) and their control (•).

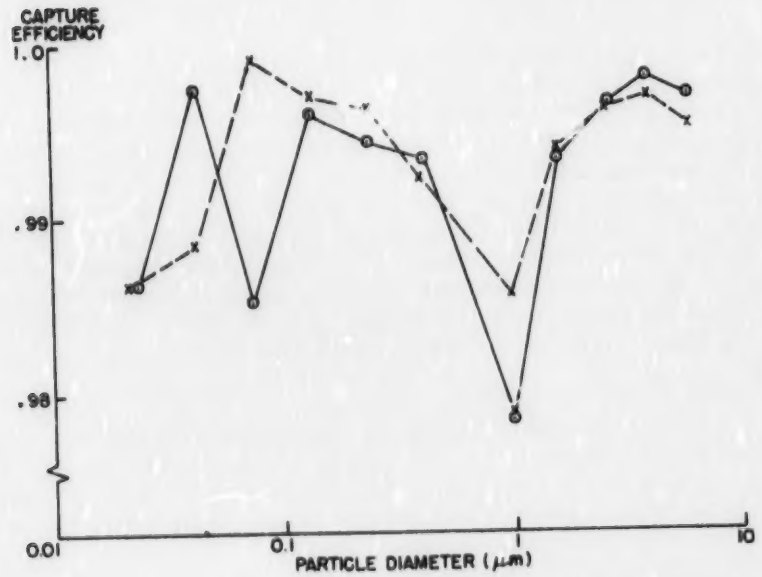

Figure 23 Twentieth-cycle capture efficiency distribution for the fabrics in Figure 22 measured with a fly-ash aerosol and allowing a cake to form. Lines serve merely to connect points; epitropic (x), control (•).

TABLE 7. PROPERTIES OF COMMERCIAL-WEIGHT FILTER SAMPLES MADE FROM POLYESTER FIBERS

	Round, smooth	Round, rough	Trilobal, rough
Wt. (oz/yd^2)	16.7	16.3	16.4
Density (g/cm^3)	0.20	0.20	0.20
ΔP_i (1) (mm H_2O)	3.0	3.5	4.0
ΔP_f (1) (mm H_2O)	28.0	26.0	27.0
K(1) (10^4 N·s/kg·m)	2.7	2.3	2.5

Capture efficiencies in the submicron region were measured without dust cake, and little difference is observed among the three samples (Figure 24). This suggests that cross-sectional shape and surface roughness do not influence the inherent capture ability of clean fabrics in the diffusion region (i.e., the particle size range below ∿0.5 μm).

Efficiencies over the entire size range were then measured using a flyash aerosol so that a cake built up. The results, shown in Figure 25, point to several conclusions:

(1) Although, for these heavier fabrics, differences in capture efficiencies for particles greater than 2.5μm are smaller than found in the previous study for 5-oz fabrics, considerable differences are still found in the submicron region.
(2) As found previously, the better efficiencies are associated with trilobal shape and rough surface.
(3) In view of the results when no cake forms (Figure 24), the differences in efficiency in the submicron region when a cake is allowed to accumulate may be attributed to differences in cake formation on the different fabrics.

In conclusion, there is no clear relationship between results obtained with filters made from fibers roughened with TiO_2 and those made from epitropic fibers. The former consistently give better capture efficiency for submicron particles when covered by a dust cake, while in the absence of dust cake, no effects are seen. With epitropic fibers there is some improvement in capture efficiency with lightweight (∿170 g/m^2) fabrics with a dust cake (Figure 20 and 21). This agrees with results obtained in the previous study of surface roughness effects [1]. However, the results obtained with flyash aerosols at commercial fabric weights (Figure 23) do not support those for (Figure 25) TiO_2-modified fiber filters.

It seems that the effects of surface roughness vary with degree of roughness as well as with the composition of the material imparting the roughness. The ability of surface asperities to capture particles and subsequently form bridges may vary with the electrical properties of a material as well as its topography. Further studies of the characterization of surface roughness are clearly necessary to elucidate and optimize the effect on filtration performance.

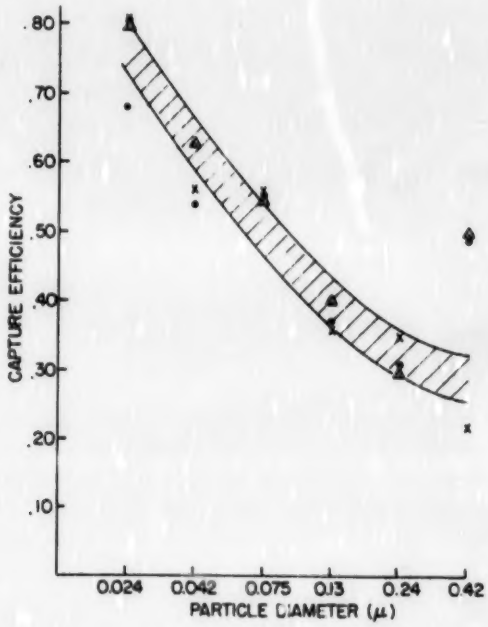

Figure 24 Capture efficiency distributions for polyester fabrics (16 oz/yd^2) measured without dust cake. Fabrics made of round, smooth fibers (•); round, rough fibers (x); and trilobal, rough fibers (Δ).

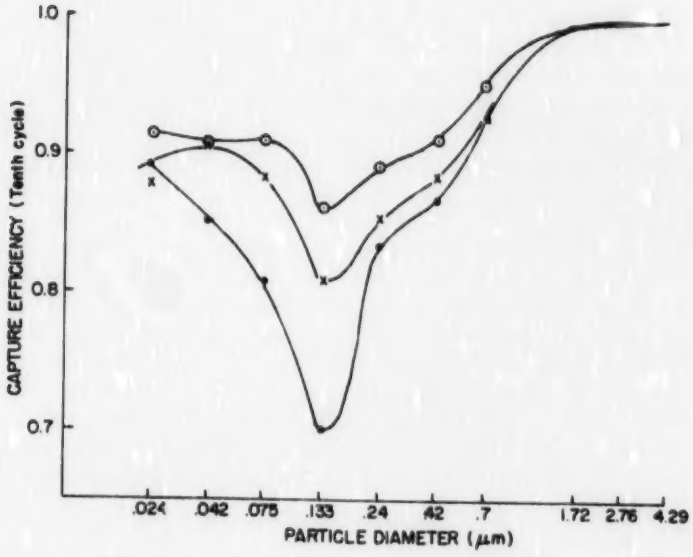

Figure 25 Capture efficiency distributions for commercial-weight filters made of round smooth (•), round rough (x), and trilobal rough (O) fibers, at the tenth cycle of filtering a flyash aerosol.

D. EFFECTS OF CRIMP

In the previous study, experiments with fabrics made of crimped and uncrimped fibers showed that the "crimped" fabrics gave higher efficiency and lower pressure drop. This information however is of limited value since in practice, uncrimped fibers are difficult to process and are therefore aimed at detecting any dependence on crimp level. This was done with two sets of fabrics. The first was made from three rayon fiber samples having crimps designated zero, normal (14.7 crimps per inch), and high (19.3 cpi). Micrographs of the three kinds of fiber are shown in Figure 26.

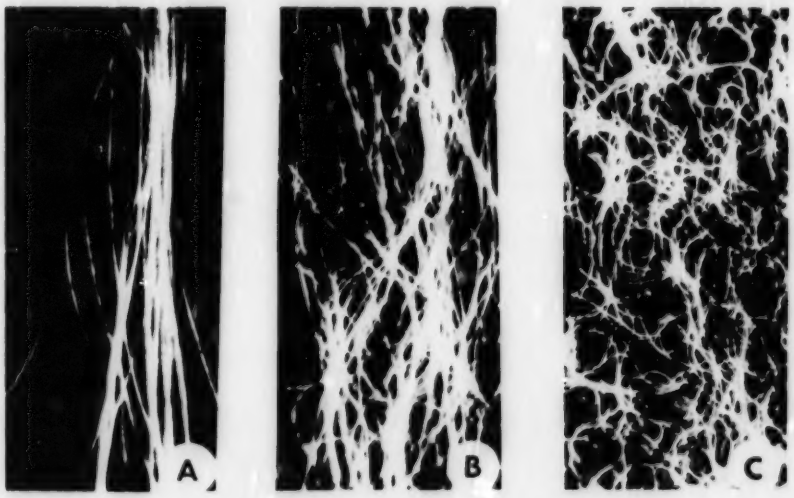

Figure 26 Micrographs of rayon fibers (12X).

A. No crimp B. Normal crimp (14.7 cpi) C. High crimp (19.3 cpi)

Efficiencies of the three fabrics (weighing 0.17 kg/m^2) were measured using atmospheric dust and no cake, and the results are shown in Figure 27. In agreement with earlier results, no differences in capture efficiencies are seen. When the fabrics were used to filter a flyash aerosol with accumulation of a dust cake, the results in Figure 28 were obtained. These show that in the presence of a cake, crimped fibers give slightly higher efficiencies than straight fibers. There is no significant advantage of high over normal crimp level, however. The advantage of crimped fibers over uncrimped extends into the diffusion region, showing again that the differences are probably due to different cake formations.

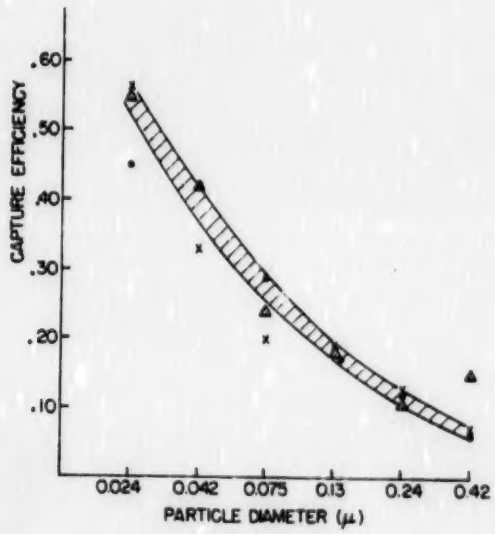

Figure 27 Capture efficiency distributions for rayon filters measured without dust cake. Filters made of fibers of three levels of crimp: 0 cpi (•), 14.7 cpi (x), and 19.3 cpi (Δ).

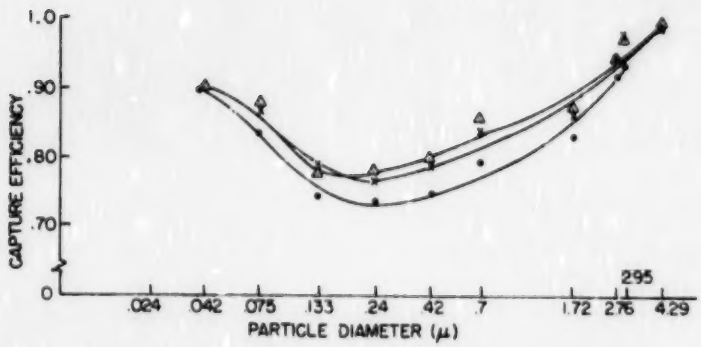

Figure 28 Capture efficiency distributions for rayon filters made with fibers at three levels of crimp: 0 cpi (•), 14.7 cpi (x), and 19.3 cpi (Δ). First-cycle efficiencies with flyash aerosol.

With regard to pressure drop characteristics, however, additional differences can be discerned. Table 8 gives results for two sets of experiments comparing the three rayon fabrics, and it can be seen that a higher crimp level brings higher air permeability and lower specific cake resistance.

TABLE 8. DEPENDENCE OF PRESSURE DROP CHARACTERISTICS ON CRIMP LEVEL FOR RAYON FABRICS

Crimps/in.	Density (g/cm^3)	K(1) (10^4 N·s/kg·m)	K(10) (10^4 N·s/kg·m)	Air permeability (ft/min)
19.3	0.112	1.63	3.85	285
14.7	0.117	1.66	3.89	276
0	0.117	1.92	4.26	210
19.3	0.112	0.99	2.17	300
14.7	0.112	1.05	2.67	282
0	0.112	1.29	3.35	252

Commercial weight fabrics ($\sim$0.5 kg/m^2) were also prepared. Because of the difficulty of preparing a web with uncrimped fibers, only the regular (14.7 cpi) and high (19.3 cpi) crimp fibers were made into Vinyon-bonded filters.

Comparisons of efficiency were made in three ways: (1) with atmospheric dust and no cake, (2) with atmospheric dust after flyash cake formation, and (3) with flyash aerosol after one and ten cycles. In the first case, as shown in Figure 29, there is once again no difference in capture efficiency without a cake. In the second case, also shown in Figure 29, there does not appear to be any difference in capture efficiency after a flyash cake is formed either. In the third case (Figure 30), in which efficiency is measured during the formation of the flyash cake on the tenth cycle, there are still no significant differences.

The effect of crimp level on pressure drop characteristics was also studied. Table 9 shows that at the tenth cycle, the final pressure drops and specific cake resistances of both high and regular crimp samples are about equal.

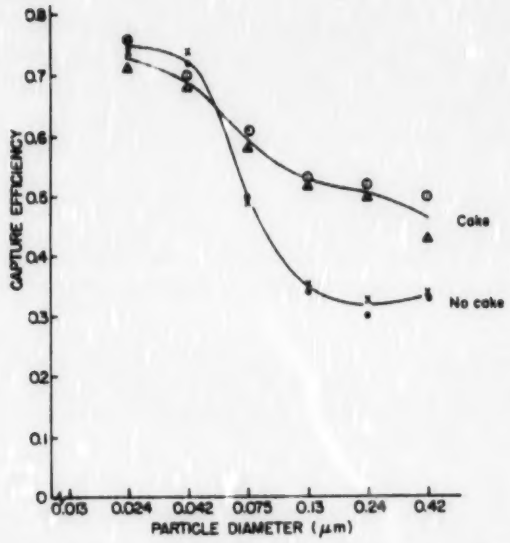

Figure 29 Comparison of capture efficiency for rayon filters made of fibers with 14.7 crimps per inch (•, ⊕) and 19.3 cpi (x, Δ) with and without dust cake. Atmospheric dust filtered through clean filter and through flyash cake.

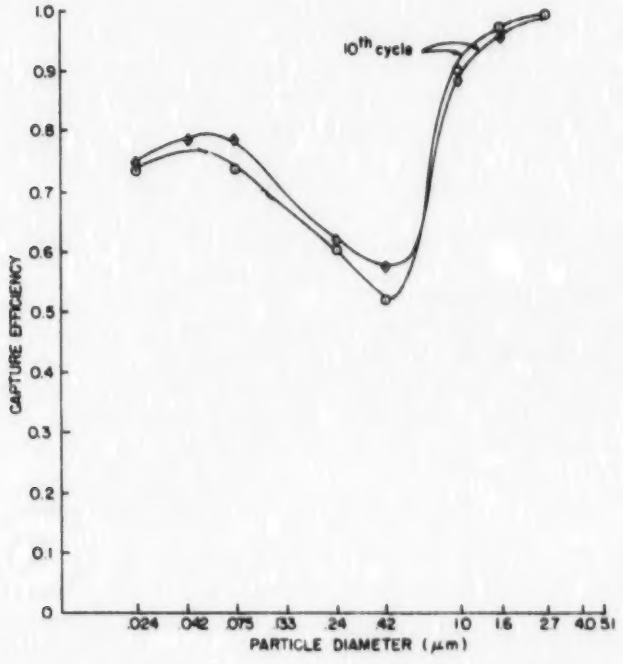

Figure 30 Capture efficiency distribution for regular (•) and high (◊) crimp rayon filters at tenth cycle.

TABLE 9. PROPERTIES OF 14-OZ RAYON FILTERS

	Crimp Level	
	Regular	High
Crimps/in.	14.7	19.3
Sample weight (oz/yd^2)	13.6	14.0
Sample density (g/cm^3)	0.155	0.151
ΔP_i (10) (mm)	3.0	2.5
ΔP_f (10) (mm)	27.0	25.0
K(10) (10^4 N·s/kg·m)	1.55	1.61
Sample weight (kg/m^2)	0.46	0.475
Face velocity (m/s)	0.061	0.061

The second set of fabrics discussed above was made from specially crimped polyester fiber. Because of the difficulty in securing a series of fibers with different levels of crimp, but differing only in that respect, a crimper was constructed, and samples of fiber with four different levels of crimp were prepared from the same feeder yarn. The crimper operated by passing the yarn between a pair of heated gears, where a wavy configuration was imparted to it, matching the gear teeth in size and frequency. Four pairs of interchangeable gears were available, giving crimp frequencies of 236, 512, 748, 1142 per meter (6, 13, 19, 29 per inch). The crimped yarn was cut into 38-mm (1.5-in.) lengths and formed into nonwoven fabrics bonded with 10% Vinyon fiber. Attempts to make a fabric from uncrimped fiber failed because of the lack of coherence in the formed web.

Performances of these fabrics in filtering a flyash aerosol are described in Table 10 and Figure 31. Results indicate no discernible trend in performance with different crimp frequencies, either in capture efficiency or in cake resistance.

TABLE 10. EFFECT OF CRIMP LEVEL IN THE PRESENCE OF A CAKE

Crimps/in.	29	19	13	6
E(10) (%)	99.63±.08	99.73± .08	99.74± .05	99.75± .04
ΔP(10) (mm H_2O)	56± 4	64± 5	65± 5	68± 13
K(10) (10^4 N·s/kg·m)	9.00±.15	9.81±1.80	9.64±2.10	8.69± .27
Air permeability (ft/min)	204± 6	190±20	181± 6	170± 9
Wt. (oz/yd^2)	6.983	7.030	6.984	6.910
Density (g/cm^3)	0.1835	0.1865	0.1800	0.1855
Face velocity (m/s)	0.061	0.061	0.061	0.061

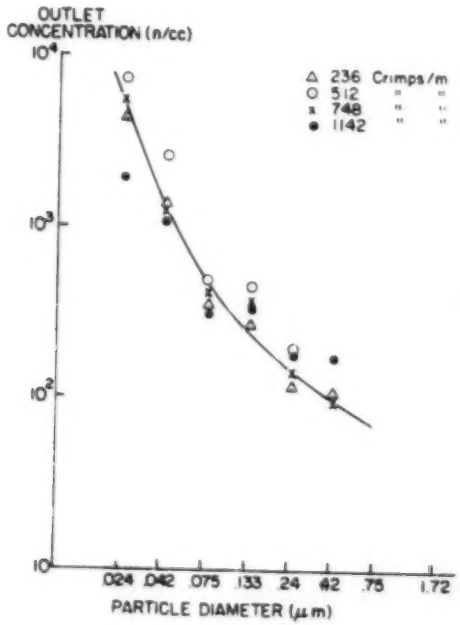

Figure 31 Outlet concentration distribution for four PET fabrics made of fibers with different crimp frequencies.

E. EFFECT OF FABRIC DENSITY

As standard procedure in all filtration performance comparisons, fabric densities have been controlled as closely as possible. All nonwovens in each test series have been made to have the same density by varying bonding pressure until thicknesses are the same for equal weights of fiber. In practice the densities obtained are usually very close to each other. However, occasionally a situation will arise in which densities do vary, but a comparison is still desired. Knowledge of the effect of fabric density on filtration performance will not only permit corrections in these situations, but will also indicate the direction for optimization of this construction variable. Accordingly, some effort has been directed to a study of the effect.

Three experiments were conducted. In the first two, clean fabric pressure drops and efficiency distributions in the submicron region using atmospheric dust were measured for two polyester fabric types at various densities. The densities were varied by compressing the fabric in a hot press at various pressures, and measurements were made after successive pressings at greater pressure. The two fabrics were: (1) a 16-oz PET (3 den) bonded with PET binder, and (2) a 16-oz PET (3 den) bonded with 10% Vinyon. The densities of the first fabric varied from 0.07 to 0.25 g/cm^3, and those of the second fabric from 0.03 to 0.27 g/cm^3. The third experiment consisted of a comparison between trilobal and round fibers in needled 13-oz nonwovens that had been subjected to different pressures to increase their original needled densities. In this case, flyash was used resulting in cake formation. Measurements were made of overall efficiency and pressure drop characteristics on the first cycle.

The results of the first two experiments are shown in Figures 32, 33, and 34, where capture efficiency and clean fabric pressure drop are plotted against packing density (the ratio of fabric density to fiber density). It can be seen from Figures 32 and 33 that for each particle size (from 0.024 to 0.24 μm) efficiency increases as packing density increases up to between 0.10 and 0.15 and then levels off. These values correspond to fabric densities between 0.14 and 0.20 g/cm^3 for polyester. In contrast, the relationship between clean fabric pressure drop and packing density at 60 mm/s face velocity (Figure 34) is linear over the same range.

The results of the third experiment (Figure 35) show the effect of fabric packing density on overall efficiency during the first cycle of flyash filtration with the needled fabrics. For both the trilobal and the round samples overall efficiency increases with increasing packing density. A leveling off apparently does not occur until beyond the last point measured (0.20).

Specific cake resistance (K) was also determined for these samples at increasing density. It can be seen in Figure 36 that K increases over the region considered and is the same for the samples made of trilobal and round fibers. This once again verifies the finding that trilobal fibers do not increase drag [1].

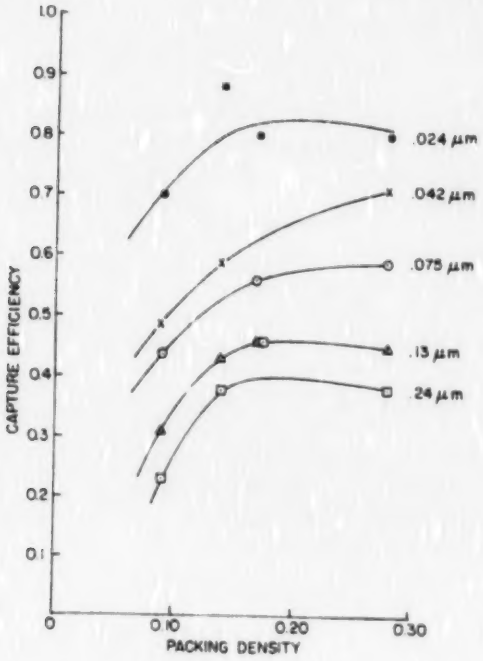

Figure 32

Effect of fabric packing density on capture efficiency for various submicron particle sizes (PET-bonded PET fabrics).

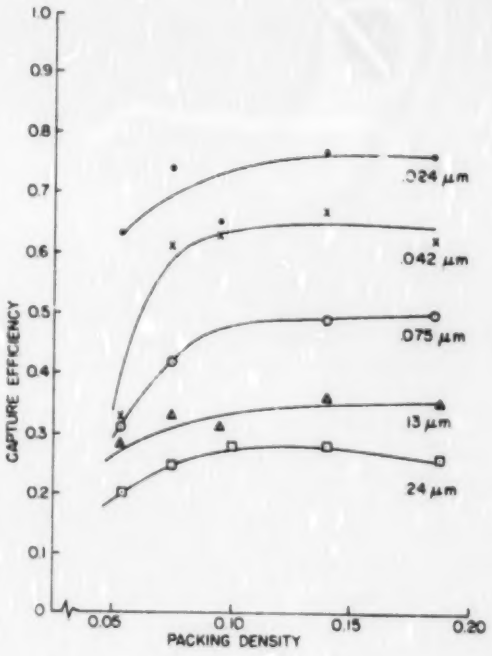

Figure 33

Effect of fabric packing density on capture efficiency for various submicron particle sizes (Vinyon-bonded PET fabrics).

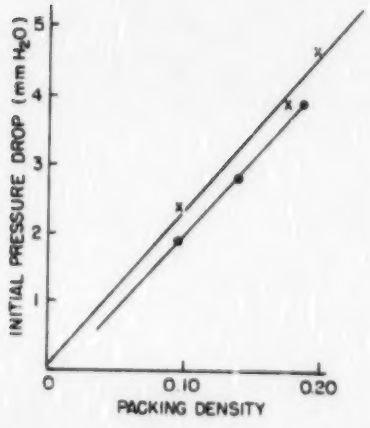

Figure 34

Effect of packing density on clean fabric pressure drop for two PET fabrics: PET-bonded (x) and Vinyon-bonded (•). Face velocity: 60 mm/s.

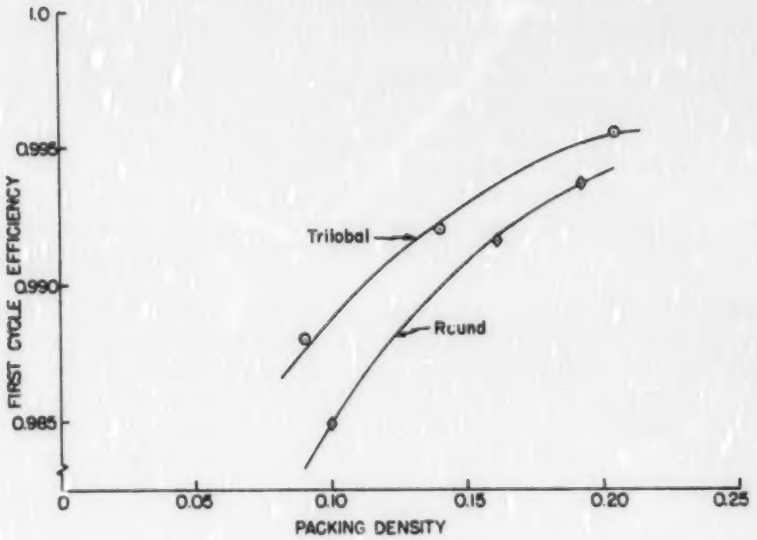

Figure 35 Effect of packing density on first-cycle efficiency for trilobal and round needled polyester fabrics.

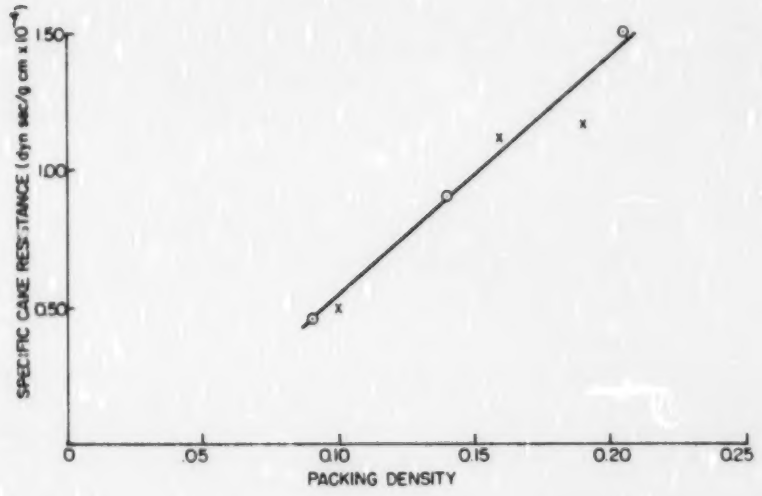

Figure 36 Effect of packing density on specific cake resistance for trilobal (•) and round (x) needled polyester fabrics.

The empirical relationship described in Section V, A, equation (2), in which efficiency was a function of d/s can be applied to the results plotted in Figures 32 and 33. These results were obtained with fabrics in which the packing density was increased by compressing the fabric. Under these circumstances packing density is inversely proportional to fabric thickness. Since the effective diameter (d) of a particle (equation 1) is proportional to the square root of the residence time in the fabric, which in turn is proportional to the fabric thickness, we find that $d \propto (\text{fabric thickness})^{\frac{1}{2}}$. But the mean fiber spacing (s) also depends on $(\text{fabric thickness})^{\frac{1}{2}}$. Therefore capture efficiency, being proportional to ln d/s, should be unaffected by fabric compression. The model therefore is consistent with the level portions of the curves (Figures 32 and 33), but fails for very low values of the packing density.

The results obtained in the presence of a dust cake must be interpreted qualitatively. Overall efficiency is dependent mainly on the bridging by larger, heavier particles. It is reasonable then to anticipate higher efficiencies as packing densities increase and interfiber spacings decrease. It is also probable that the cakes formed on higher density fabrics are more compact and less porous, which accounts for the increased cake resistance shown in Figure 36.

F. RESULTS OF BAGHOUSE TRIALS

In order to verify bench-scale results on a larger scale, experiments were performed with a one-bag baghouse. It was necessary first to construct the baghouse, as described in Section IV, C, and then to fabricate bag fabrics from the proper fibers. This was done on commercial machinery by sandwiching a scrim between two card webs and then needling the assembly to the correct density. The fabrics were then fashioned into bags. Five such fabrics were obtained, and they are described in Table 11.

TABLE 11. SPECIALLY MADE NEEDLED POLYESTER FABRICS

Bag Fabric No.	Linear density (den)	Surface	Shape	Crimp
A	3	Smooth	Round	Yes
B	3	Smooth	Trilobal	Yes
C	6	Rough	Round	No
D	6	Smooth	Round	No
E	6	Smooth	Trilobal	No

Bag Trial - Effect of Cross-Sectional Shape (3-den fibers)

For a first comparison bags A and B (3 den) were conditioned for 50 5-min cycles, after which conditions appeared to have reached a steady state. The outlet concentrations (C_o) were sampled over a further 10-cycle period, and the initial and final pressure drops were recorded. This was done at face velocities of 15, 30, 45 and 60 mm/s (3, 6, 9 and 12 ft/min) and at a constant inlet concentration of 8.5 g/m^3. In order to ensure constant inlet concentrations at these different flow rates, a preliminary set of experiments had to be made, in which inlet concentrations were measured over a range of feeder settings and flow rates. This allowed selection of the desired inlet concentration by adjusting the feeder to the proper setting (See Figure 5).

The results are shown in Figures 37 and 38 and Table 12. In Figure 37 the "trilobal" fabric is shown to give consistently lower pressure drops over the range of face velocities studied. This presure drop advantage, which is about 20%, was not observed in experiments done with patch filters. The reason may lie in the different cleaning methods, i.e., reverse air with no shaking for the patch filters vs. pulse jet for the bag.

TABLE 12. OUTLET CONCENTRATIONS FOR TRILOBAL AND FOR ROUND FIBER FILTER BAGS AT VARIOUS FACE VELOCITIES

(Inlet concentration constant at 8.5 g/m^3; cycle time constant at 5 min.)

Particle size (μm)	Outlet concentrations (Trilobal/Round) (Samples B vs. A) (particles/cm^3) x10^3			
	at 15 mm/s	at 30 mm/s	at 45 mm/s	at 60 mm/s
.013	2.13/12.53	4.16/16.00	2.78/3.48	0.68/ 4.87
.024	0.84/ 4.19	1.70/ 5.30	1.12/2.79	0.00/ 3.07
.042	0.44/ 2.32	1.02/ 1.89	0.87/1.31	0.87/ 0.29
.075	0.81/ 1.55	1.25/ 1.41	0.89/1.26	1.64/ 1.92
.133	0.96/ 2.08	1.36/ 1.84	0.85/1.88	2.07/ 2.44
.24	0.44/ 1.16	0.53/ 0.95	0.27/0.82	1.04/ 1.79
.42	0.34/ 0.84	0.34/ 0.67	0.17/0.50	0.67/ 1.40
0.5	7.70/ 6.53	4.48/ 3.67	1.22/ 5.31	6.94/10.20
1.0	2.47/ 4.75	2.30/ 3.11	1.27/ 2.65	3.54/ 4.85
1.6	1.04/ 2.16	0.76/ 1.32	0.53/ 1.02	1.43/ 2.07
2.7	0.26/ 0.73	0.22/ 0.35	0.14/ 0.33	0.48/ 0.64
4.0	0.061/0.169	0.055/0.080	0.035/0.068	0.104/0.150
5.1	0.024/0.049	0.018/0.023	0.010/0.023	0.028/0.041

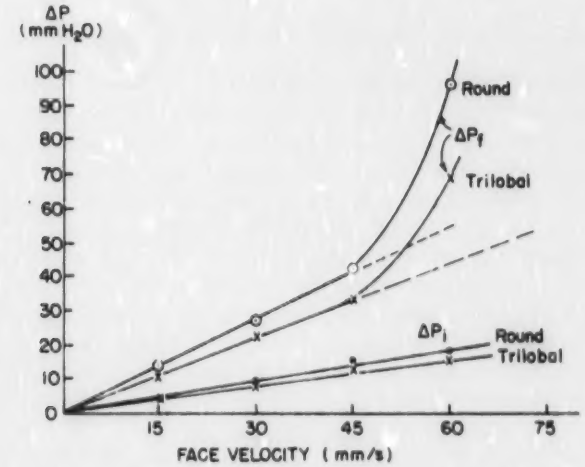

Figure 37 Initial (ΔP_i) and final (ΔP_f) pressure drops obtained with bags made of trilobal and round cross section fibers.

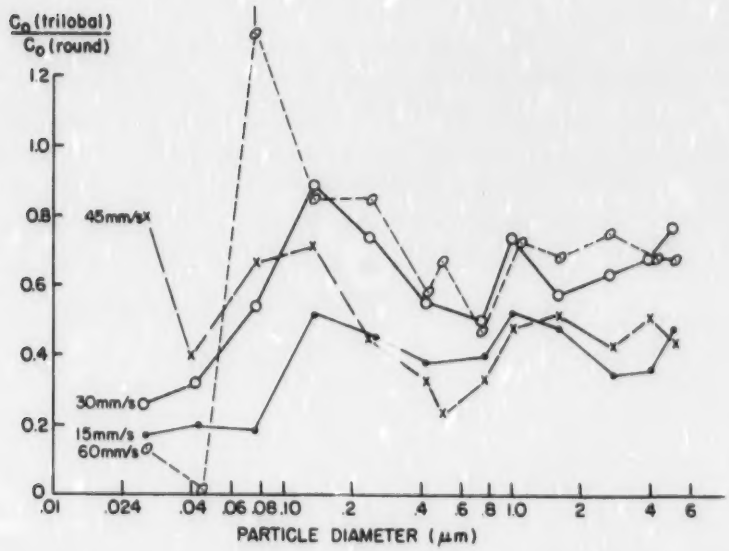

Figure 38 Ratio of C_0 for a PET filter bag made of trilobal fibers to C_0 for a round-fiber bag as a function of particle diameter at several face velocities (Table 12).

The effect on capture efficiencies is shown in Table 12 for the four face velocities and for the range of particle sizes covered by our equipment. The results are expressed as the ratio of penetration for the trilobal to the round cross-section bag. Since most of the ratios are <1, trilobal bags are seen to give consistently better efficiency. The ratios in Table 12, when plotted (Figure 38), yield curves that reveal no significant dependence of the efficiency ratio on either face velocity or particle size. Rather there is a rather diffuse clustering of the values in the neighborhood of 0.5, so that the results may be summarized by saying that the "trilobal" fabric gives one half the penetration of the "round" fabric.

The second part of the evaluation was made with bags C, D, and E. Owing to a misunderstanding, uncrimped fibers were used to fabricate the cloth for these bags. This caused some difficulties and is assumed to be the reason for the nonuniformities in weight and thickness which were found to be greater for these three fabrics than for fabrics A and B. The extent of these nonuniformities is indicated in Table 13, which lists averages obtained for 10 pieces, 12.5 cm x 12.5 cm, cut from each of the fabrics. The differences in fabric weight were reduced by cutting each fabric into a number of pieces, each of the correct size for making one bag. The pieces were weighed and bags made from pieces that were closest in mass. The masses of the three pieces selected were 228, 223, and 223 g, which could be regarded as essentially identical. This procedure, however, could not reduce the differences in density between fabrics which can be seen from Table 13 to be appreciable. To provide a measure of the effect of these density differences, a series of supporting experiments were made with patch-size (12.5 cm x 12.5 cm) samples of fabrics C, D, and E, in which the effects of different packing densities were revealed by compressing the fabrics under heat. Results of these measurements may be used to estimate what the results of the bag trials would have been if packing densities had been the same for all fabrics.

TABLE 13. VARIATIONS IN WEIGHT, THICKNESS, DENSITY, AND STANDARD FRAZIER AIR PERMEABILITY OF BAG FABRICS LISTED IN TABLE 11

Bag Fabric No.	Weight ± σ (g/m^2)	Thickness ± σ (mm)	Density (g/cm^3)	A.P. ± σ (cm/s)
A	442± 6	3.18±.06	0.076±.002	51± 3
B	440±10	3.44±.08	0.070±.001	48± 3
C	459±18	2.29±.08	0.109±.002	60±11
D	397±21	2.70±.14	0.080±.003	93±14
E	449±19	3.43±.07	0.071±.002	78± 7

Again, each bag was conditioned with flyash for at least 50 cycles before filtration performance evaluations. Inlet concentration was kept at 8.5 g/m^3. Outlet concentrations and pressure drops as reported are averages for 10 cycles.

Bag Trial - Effect of Surface Roughness

The comparison of bags C and D was made questionable from the outset by the large difference in fabric density shown in Table 13. The difference in fabric density is due to the different response of rough fibers to the fabrication procedure. Fabrics C, D, and E were made by the following identical procedure: 6 oz/yd^2 laps were needled into a 10 x 10 PET scrim in a four-pass operation. The first lap was punched at 500 punches/in.^{2} onto one side of the scrim and the second lap similarly on the other side. Side one was then again punched at 500 punches/in.^{2} and so was side two. The different frictional properties of the rough fibers resulted in a much more compact structure. Weight variations shown in Table 13 are about twice as large for samples C, D, and E than for samples A and B. Air permeabilities (A.P.) vary by three times as much.

With the density of the rough fabric about 30% higher than that of the smooth fabric, it would be expected *a priori* that the rough fabric would give higher efficiency and pressure drop by virtue of its higher density alone. This would mask any improvement in performance that might be due to the rough fiber surfaces. The only value in performing this comparison, therefore, is to verify the above expectations. Should the reverse be observed, then it would indicate a strong reverse effect due to surface roughness, an unlikely event in view of the findings in previous sections of the present report. Table 14 lists the ratios of rough-to-smooth fabric outlet concentrations for a range of particle sizes and pressure drops [$\Delta P = (\Delta P_f - \Delta P_i)$] for each fabric. The results indicate that in fact the efficiencies and pressure drop for the rough fabric are higher, as expected. Under these conditions, it is necessary to resort to the secondary measurements reported later in this section for confirmation of the slightly better performance of the needled rough-fiber fabric.

TABLE 14. OUTLET CONCENTRATIONS AND PRESSURE DROPS FOR ROUGH AND SMOOTH-FIBER FILTER BAGS AT VARIOUS FACE VELOCITIES

(Inlet concentration kept constant at 8.5 g/m^3; cycle time constant at 7.5 min.)

Particle size (μm)	Outlet concentration (Rough/Smooth) (Samples C vs. D) (particles/cm^3) x 10^3		
	at 15 mm/s	at 30 mm/s	at 60 mm/s
.013	4.93 / 5.60	4.87 /4.87	2.82 /6.26
.024	2.23 / 2.79	2.51 /2.79	2.36 /4.46
.042	0.73 / 1.45	0.73 /1.45	0.29 /0.29
.075	0.59 / 1.48	0.60 /0.96	1.18 /1.85
.133	0.84 / 1.56	0.72 /1.24	1.20 /2.40
.24	0.36 / 0.55	0.29 /0.61	0.51 /1.18
.42	0.22 / 0.34	0.062/0.11	0.37 /0.78
0.5	4.93 /10.07	4.90 /6.80	3.44 /6.25
1.0	3.71 / 6.50	3.83 /4.97	2.31 /3.78
1.6	1.73 / 2.58	1.61 /1.73	0.88 /1.07
2.7	0.49 / 0.77	0.48 /0.48	0.28 /0.34
4.0	0.12 / 0.17	0.42 /0.35	0.070/0.089
5.1	0.038/ 0.060	0.038/0.039	0.022/0.022
	($\Delta P_f - \Delta P_i$) (Rough/Smooth)		(mm H_2O)
	13/9	37/23	82/53

Bag Trial - Effect of Cross-Sectional Shape (6-den fibers)

The comparison of bags D and E (6 den) presented a problem similar to that of the previous comparison, but here the difference in the fabric densities was only about 12%, being higher for the "round" fabrics. In the absence of other effects, the higher density of the "round" fabric should therefore result in higher efficiency and pressure drop than for the "trilobal" fabric. Table 15 indicates an opposite trend with respect to efficiency, which is higher for the trilobal fabric, for particles greater than 0.5 μm. For particles smaller than 0.5 μm, the efficiency was higher with the round fabric. This peculiar crossover was not explained. The overall mass efficiency is determined by the behavior of the larger particles, so that the results in Table 15 agree with those in Figures 39 and 40.

Pressure drops (Table 15) are about equal for the two bags, indicating that if fabric densities had been equal, the trilobal bag would have scored worse in this respect. The overall performance of the trilobal bag may, however, be taken to be better than that of the round bag from the data obtained. The pressure drops recorded in Table 15 are differences between pressure drops measured

at the beginning and end of each cycle. It would therefore be misleading to attempt to calculate specific cake resistance from these values, since the pressure drop increased rapidly at the beginning of a cycle, owing to redeposition which is characteristic of pulse-jet cleaned bags. In addition, the amount of redeposited dust would be expected to vary with face velocity.

TABLE 15. OUTLET CONCENTRATIONS AND PRESSURE DROPS FOR TRILOBAL AND FOR ROUND FIBER FILTER BAGS AT VARIOUS FACE VELOCITIES

(Inlet concentration constant at 8.5 g/m^3; cycle time constant at 7.5 min.)

Particle size (μm)	Outlet Concentration (Trilobal/Round) (Samples E vs. D) (particles/cm^3) x 10^3			
	at 15 mm/s	at 30 mm/s	at 45 mm/s	at 60 mm/s
0.013	8.35 / 5.60	2.09 /4.87	7.66 /0.70	2.75 /6.26
0.024	4.46 / 2.79	1.67 /2.79	4.45 /3.91	3.62 /4.46
0.042	1.31 / 1.45	0.73 /1.45	0.44 /0.44	1.31 /0.29
0.075	1.33 / 1.48	2.88 /0.96	1.78 /0.89	1.26 /1.85
0.133	2.18 / 1.56	2.00 /1.24	1.88 /1.48	1.44 /2.40
0.24	1.20 / 0.55	0.84 /0.61	0.90 /0.74	0.56 /1.18
0.42	1.07 / 0.34	0.21 /0.11	0.56 /0.39	0.39 /0.78
0.5	9.76 /10.07	5.17 /6.80	6.51 /6.25	4.38 /6.25
1.0	5.72 / 6.50	4.22 /4.97	3.98 /4.18	2.98 /3.78
1.6	2.48 / 2.58	1.53 /1.73	1.22 /1.36	0.85 /1.07
2.7	0.70 / 0.77	0.40 /0.48	0.33 /0.40	0.27 /0.34
4.0	0.16 / 0.17	0.30 /0.35	0.085/0.101	0.069/0.089
5.1	0.047/ 0.060	0.027/0.039	0.023/0.029	0.019/0.022
	$(\Delta P_f - \Delta P_i)$ (Trilobal/Round) (mm H_2O)			
	11/9	22/23	38/35	50/51

Supporting Bench-Scale Measurements

In a further series of trials, the variations in fabric density between samples C, D, and E were eliminated by selecting patches of equal weight and pressing them at 100°C to various thicknesses to give a range of densities. Samples given this treatment were found to be quite stable during conditioning for 15 cycles and subsequent measurement. Values of E and K as a function of packing density are then given for both 30 and 60 mm/s (6 and 12 ft/min) in Figures 39, 40, and 41. It can be seen that trilobal smooth fiber filters remain more efficient than round smooth fiber filters over a wide range of packing densities at both face velocities (Figures 39 and 40). Round rough fiber filters were not pressed, since they already were

high in density. Efficiency data points (marked A) for round rough samples can be seen to be higher than those for round smooth samples at the same packing densities.

Cake resistance as a function of packing density is plotted for both face velocities in Figure 41. Least-squares fits show that K for trilobal fiber filters is not significantly different from that for round fiber filters either at 60 or at 30 mm/s. K values for rough fiber filters (data points marked A) are lower than or equal to those for their smooth-fiber counterparts.

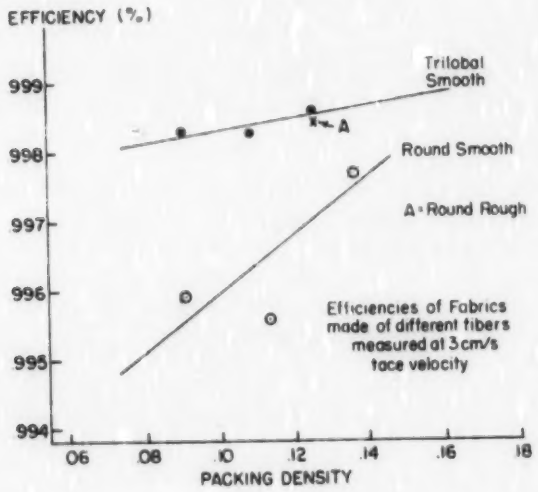

Figure 39

Efficiency of PET patch filter fabrics as a function of packing density at a face velocity of 30 mm/s.

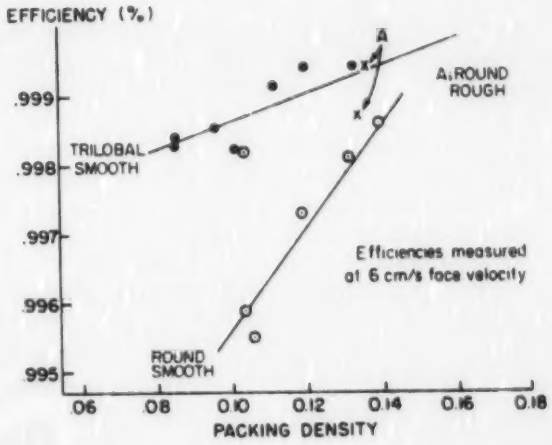

Figure 40

Efficiency of PET filter fabrics as a function of packing density at a face velocity of 60 mm/s.

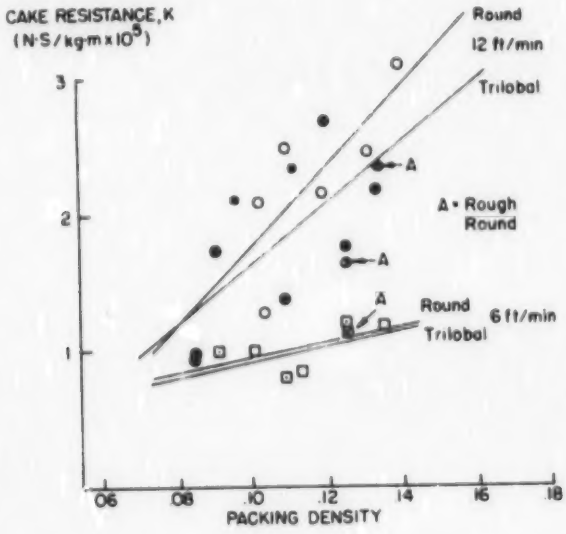

Figure 41 Cake resistance of PET filter fabrics as a function of packing density at the two face velocities, 30 (round o, trilobal ·) and 60 (round □ trilobal ⊡) mm/s (6 and 12 ft/min).

SECTION VI

REFERENCES

1. Miller, B., Lamb, G.E.R., and Costanza, P., "Influence of Fiber Characteristics on Particulate Filtration," Office of Research and Development, USEPA, Publication No. EPA-650/2-74-043, May 1974.

2. Thornley, W. R., Operating Manual, AIR Model 30 Aerodynamic Particle Sizer, AIR, Inc., Logan, Utah, 1971.

3. Loeb, L. D., "Kinetic Theory of Gases," McGraw-Hill Book Co., New York, 1934.

4. Spielman, L. and Goren, S. L., Model for Predicting Pressure Drop and Filtration Efficiency in Fibrous Media, Environmental Sci. and Tech. 2, 279-287 (1968).

5. Brinkman, H. C., A Calculation of the Viscous Force Exerted by a Flowing Fluid on a Dense Swarm of Particles, Appl. Sci. Res. A1, 27-34 (1947).

6. Ellis, V. S., EPITROPIC - Third Generation Conductive Fibers, Textile Manufacturer 101, No. 1193, pp. 19-23, July 1974.

SECTION VII

CONVERSION TABLE

Physical Quantity	To convert from	to	multiply by
Crimp frequency	crimps/m	crimps/in.	0.0254
Face velocity	ft/min	air-to-cloth ratio	1
Face velocity	cm/s	ft/min	2
Mass per unit area	kg/m^2	oz/yd^2	29.5
Concentration	g/m^3	$grains/ft^3$	0.437